arXiv:astro-ph/0204430v1 25 Apr 2002

Near-Infrared Photometric Variability of Stars Toward the Chamaeleon I Molecular Cloud

John M. Carpenter, Lynne A. Hillenbrand

California Institute of Technology, Department of Astronomy, MS 105-24, Pasadena, CA 91125

jmc@astro.caltech.edu, lah@astro.caltech.edu

M. F. Skrutskie[1]

University of Massachusetts, Department of Astronomy, Amherst, MA 01003

mfs4n@virginia.edu

and

Michael R. Meyer

University of Arizona, Steward Observatory, Tucson, AZ 85721

mmeyer@as.arizona.edu

ABSTRACT

We present the results of a J, H, and K_s photometric monitoring campaign of a $0.72^\circ \times 6^\circ$ area centered on the Chamaeleon I star forming region. Data were obtained on 15 separate nights over a 4 month time interval using the 2MASS South telescope. Out of a total of 34,539 sources brighter than the photometric completeness limits (J=16.0, H=15.2, K_s=14.8), 95 exhibit near-infrared variability in one or more bands. The variables can be grouped into a population of bright, red objects that are associated with the Chamaeleon I association, and a population of faint, blue variables that are dispersed over the full 6° of the survey and are likely field stars or older pre-main-sequence stars unrelated to the present-day Chamaeleon I molecular cloud. Ten new candidate members of Chamaeleon I, including 8 brown dwarf candidates, have been identified based on variability and/or near-infrared excess emission in the $J-H$ vs. $H-K_s$ color-color-diagram. We also provide a compendium of astrometry and J, H, and K_s photometry for previously identified members and candidate members of Chamaeleon I.

[1]Current Address: University of Virginia, Department of Astronomy, P.O. Box 3818, Charlottesville, VA 22903

Subject headings: infrared: stars — stars:pre-main-sequence — stars:variables — open clusters and associations

1. Introduction

Near-infrared variability provides a means to identify young stellar populations independent of most current observational selection techniques (e.g. Hα, Li, x-ray, and near-infrared excess surveys), and has been shown to be sensitive to stars both with and without circumstellar accretion disks (Skrutskie et al. 1996). Variability studies, therefore, help provide a more complete census of the stellar population in star forming regions. In the first (Carpenter, Hillenbrand, & Skrutskie 2001, hereafter CHS01) of a series of papers on the near-infrared photometric variability properties of pre-main-sequence objects, we analyzed J, H, and K_s time-series data of nearly 18,000 stars distributed over a $0.84^\circ \times 6^\circ$ region toward the Orion A molecular cloud using observations conducted with southern 2MASS telescope. The vast majority of the $\sim$1200 stars with time-variable $\mathrm{JHK_s}$ photometry identified in that study are young pre-main sequence stars associated with the Orion molecular cloud. The large sample of variables was used to investigate the characteristics and origins of near-infrared variability in young stars.

A diversity of photometric behavior was observed during the $\sim$30-day time period encompassed by the Orion observations, including cyclic fluctuations, eclipses, aperiodic short-term fluctuations, slow drifts in brightness over the full length of the observing period, colorless variability, stars that become redder as they fade, and stars that become bluer as they fade. Rotational modulation by cool spots alone can explain the observed variability characteristics in $\sim$56-77% of the stars, while the properties of the photometric fluctuations are more consistent with hot spots or extinction changes in at least 23% of the stars, and with variations in the mass accretion rate or inner radius changes in the disk in $\sim$1% of the stars.

One limitation of the Orion survey is that at the distance of the Orion molecular cloud, the flux-limited observations were most sensitive to variability in stars more massive than $1\,\mathrm{M}_\odot$. Observations of more proximate regions can use variability as a probe of lower mass stars and substellar objects and establish if the variability characteristics vary as a function of mass. Accordingly, we have conducted a near-infrared monitoring campaign of the Chamaeleon I star forming region. At a distance of 160 pc (Whittet et al. 1997), Chamaeleon I is three times closer than the Orion molecular cloud, and contains a moderately large sample of young pre-main sequence stars ($\sim$120) that have already been identified (see Lawson, Feigelson, & Huenemoerder 1996 and references therein). Using the 2MASS south telescope, we observed a $0.72^\circ \times 6^\circ$ region centered on the Chamaeleon I molecular cloud on 15 nights over a 4 month time period. These observations monitored over 34,000 stars with sensitivity to detect variability in young brown dwarfs with masses as low as $\sim 0.05\,\mathrm{M}_\odot$.

The observations and data reduction procedures for this data set are described in Section 2. In Section 3, we identify the variable stars from the time series photometry, present light curves for

all of the variable stars, and examine the spatial distribution and near-infrared photometric characteristics of the variable population. In Section 4, we identify candidate members of Chamaeleon I based on near-infrared variability and also near-infrared excesses inferred from the time-averaged photometry. Our conclusions are summarized in Section 5. A list of near-infrared photometry of known and candidate members of Chamaeleon I is provided in the Appendix.

2. Data

2.1. Observations and Data Processing

The observing and data reduction procedures for the Chamaeleon I data closely follow that used in the Orion variability study. This section summarizes aspects of the data relevant specifically to the Chamaeleon I data. A more complete description of the data processing procedures can be found in CHS01 and Cutri et al. (2000).

The J, H, and K_s observations of Chamaeleon I were obtained with the 2MASS 1.3 meter telescope at Cerro Tololo, Chile near the completion of the southern survey operations when auxiliary projects were scheduled in otherwise idle telescope time. All data were collected in standard 2MASS observing mode by scanning the telescope in declination to cover tiles of size $(\Delta\alpha \times \Delta\delta) \sim (8.5' \times 6^\circ)$ in the three bands simultaneously. The nominal region surveyed for this project consists of eight contiguous tiles in right ascension as listed in Table 1, with each tile centered on declination -77°. The total sky coverage is $\sim 0.72^\circ \times 6^\circ$. Observations were obtained on 15 separate nights, 13 of these in April and May, 2000, and 2 in January 2000 when Chamaeleon I was observed as part of the normal 2MASS survey operations covering the entire sky. Complete coverage of all 8 tiles was obtained on 9 separate nights, while scheduling constraints limited observations to a subset of the eight tiles on the other 6 nights.

Adjacent tiles overlap by at least $40''$ in the 2MASS observing procedure to ensure complete coverage of the sky as well as a check on the photometric repeatability of the observations. In practice, since the telescope is stepped slightly in right ascension while scanning a tile in declination, the amount of right ascension overlap changes with declination. For low declination regions such as Chamaeleon I, there is near complete overlap at the southernmost declinations within a tile in order to maintain the minimum overlap in the north. Thus for a large fraction of the sources there is more than one measurement per night. Of the sources meeting the photometric completeness limits described in the following section, 53% have 12-14 photometric measurements, 38% of have 23-25 measurements, and the rest mainly have intermediate number of measurements due to photometric incompleteness and nights with partial coverages.

The data were reduced using a development version of the 2MASS data processing pipeline at the Infrared Processing and Analysis Center (IPAC) that also generated the data products for the 2MASS first and second incremental release catalogs. The data discussed in this paper though were

not part of these incremental releases and will ultimately be replaced by the results of the final 2MASS processing. The 2MASS Explanatory Supplement (Cutri et al. 2000) contains complete details of the IPAC data reduction procedures. As with the Orion data, the photometric zero point was adjusted by us for each tile using bright, isolated stars as secondary standards (see CHS01 for full description of the methods). On a few scans, the photometric offsets derived from the secondary standards deviated systematically from the mean offset by up to 0.1-0.2 magnitudes over a $\Delta\delta \sim 0.5^\circ$ region of the 6° long tile. These photometric deviations are presumably caused by clouds passing overhead. For the affected region within a scan, the photometric offsets as a function of declination were computed by averaging the offsets for every 10-15 secondary standards. Photometric offsets were derived in this manner for portions of 13 scans out of a total of 108 scans observed for this project, and affected only $\sim 1\%$ of the total scan area.

2.2. Point Source List

As a first step in generating the point source list, we established the photometric completeness limit of the observations. Using data from the 9 nights on which all eight tiles were observed (see Table 1), we empirically determined the magnitude limit at which a star is expected to be detected on at least 8 of the 9 nights in the absence of source confusion. The lack of a detection on the one night can be attributed typically to random noise that puts the star below the sensitivity limit of the observations. The completeness limit as defined here then is the magnitude at which there is a 89% chance that the star was detected on an appropriate apparition. This magnitude limit occurs at approximately J=16.0, H=15.2, and K_s=14.8 for these data, corresponding to a signal-to-noise ratio of ~ 7 as discussed below.

Our initial point source list, generated from the 9 nights in which all tiles were observed, contained 34,539 sources each having an average magnitude brighter than or equal to the photometric completeness limit in at least one band. Of these, $\sim 96\%$ have no artifact or confusion flags from the processing pipeline in any of the observations. After removing those sources flagged as persistence or filter glints, potential lingering artifacts were identified as objects that had unusually blue colors for stars, were detected less than 8 times, or had flags indicating contaminated or confused photometry from a nearby star. Many of these 1266 sources were visually inspected in the images, and sources deemed as artifacts were then removed from the point source list. Criteria were established from this exercise to identify and remove likely artifacts for those sources not examined individually. Of the 34,539 stars meeting the magnitude completeness criteria, only 185 were deemed artifacts. The final source list for our variability analysis therefore contains 34,354 stars brighter than the defined completeness limits (J=16.0, H=15.2, K_s=14.8) in at least one band. Compared to the Orion observations (CHS01), Chamaeleon I contains nearly twice the number of sources (34,354 vs. 18,552) since it is both closer to the galactic center ($l = 297^\circ$ vs. 209°) and the galactic plane ($b = -16^\circ$ vs. -19°). However, the number of sources removed as artifacts is 4 times lower (185 vs.

744) since Chamaeleon I does not have the combination of high stellar density and bright nebulosity that makes photometry and source identification difficult in Orion.

To estimate the signal to noise of the photometry, Figure 1 shows the observed photometric RMS in the time series for each star as a function of magnitude. As discussed in CHS01, suspect photometric measurements for stars that are extended at the 2MASS resolution or have a high reduced chi-squared from a single PSF measurement were excluded when computing the RMS. Figure 1 shows a correlation with magnitude as expected if the observed RMS in the time series is due for the bulk of the stars to photometric noise and not due to intrinsic variability. The observed RMS values range from a minimum of ~ 0.020 mag for the bright stars to $\lesssim 0.15$ mag for stars near the completeness limit. The observed RMS floor of ~ 0.020 mag for the brighter stars is interpreted as the minimum photometric repeatability for these data, and consequently, a minimum photometric uncertainty of 0.020 mag has been imposed on all of the photometric measurements. Based upon the estimated photometric uncertainties produced by the IPAC data reduction pipeline, we find that 99%, 90%, 80% of the stars brighter than the respective completeness limits at J, H, and K_s have a signal to noise ratio per measurement ≥ 10, and 99% have a signal to noise ratio ≥ 7.

3. Variable Stars in the Chamaeleon I Molecular Cloud

3.1. Identification

Operationally, we define as a variable any star that exhibits larger photometric variations over the course of a time series than expected based upon the photometric uncertainties. Following CHS01, we used the Stetson statistic (Stetson 1996), which correlates the photometric fluctuations observed in J, H, and K_s bands, as our primary means to identify candidate variable stars. As a secondary indicator, we also identified stars that have large reduced chi-squared in the time series data but otherwise small Stetson index. The light curves and images for each candidate variable star were visually examined; 17 stars were removed and 12 stars that had a high reduced chi-squared but otherwise low Stetson index were added. The final list contains 95 variable stars.

Figure 2 shows the Stetson statistic (S) as a function of the H-band magnitude. For random noise, the Stetson variability index should be scattered around zero, and have higher, positive, values for stars with correlated variability. As in the Orion analysis, the Stetson variability index for the Chamaeleon I objects has a positive value on average for brighter stars. The origin of this offset is unclear, but is suggestive of a weak correlation between the J, H, and K_s photometry, possibly due to the fact that the three bands are observed simultaneously at each point in the time series. The minimum value of the Stetson variability index which likely represents real photometric variability, as opposed to random noise, was estimated by plotting the Stetson index versus the observed χ^2_ν, and also from visual examination of the light curves as a function of the Stetson index. Variable stars were defined based on this analysis as objects having Stetson index $S \geq 1.00$. This

threshold is larger than the value used for the Orion observations ($S = 0.55$) since the Orion data contained more photometric observations and consequently exhibited smaller scatter in the Stetson index.

Table 3 summarizes the photometric properties of the 95 variable stars identified from our data. Included in the table are an ID number, a common name for previously identified variable stars, the equatorial J2000 coordinates, the average J, H, and K_s magnitudes, the observed photometric RMS, the number of high quality photometric measurements used to assess the variability, and the Stetson variability index.

3.2. Light Curves

To illustrate the data obtained for this study, Figure 3 presents time-series photometry for the variable star 11344 (also known as T 29 and Sz 22). This figure shows the J, H, and K light curves, the K_s vs. $H - K_s$ color-magnitude diagram, and the $J - H$ vs. $H - K_s$ color-color diagram. The electronic version of this article contains figures similar to Figure 3 for all 95 variable stars, but which also include the $J - H$ and $H - K_s$ light curves, the J vs. $J - H$ color-magnitude diagram, postage stamps of the J, H, and K_s images, and a tabular summary of the photometric data. Further, `.gif` images of these figures, links to tabular data, and cross references to existing optical and near-infrared catalogs are also currently available at the web site http://www.astro.caltech.edu/∼jmc/variables/cham1.

As with the Orion observations, the variable stars in the Chamaeleon I dataset show a diversity of behavior including: gradual increases or decreases in the stellar brightness over the course of the time series observations, decreases in the brightness on discrete days that may indicate an eclipsing system, colorless fluctuations, and instances where the colors become redder as the star fades. (Periodic variables were also identified in the Orion study but a similar time-series analysis was not performed on the Chamaeleon I data due to the more limited, coarser time sampling.)

Most of the Chamaeleon I variables do not exhibit color variations with the brightness fluctuations. However, 14 of the variables exhibit observed dispersions in $J - H$ and $H - K_s$ colors more than 1.5 times larger than expected based on photometric noise. Figure 3 shows one example of color variability, which may be caused by either extinction variations or hot spots on the stellar surface (CHS01). After considering that up to half of the variable stars in Chamaeleon I may be field stars (see Sections 3.3 and 3.4), we conclude that ∼15-30% of the variables associated with Chamaeleon I show color variability. Similarly, 23% of the Orion variables show color variations of this type. No stars in Chamaeleon I become bluer as they dim, which is consistent with the results in Orion where only 1% of the variables exhibited these characteristics.

3.3. Spatial Distribution of the Variable Stars

The spatial distribution of variable stars identified in this study is presented in Figure 4. Also shown for comparison are (1) all sources in our point-source list with $J \leq 16.0$, (2) sources with a near-infrared excess detectable in the $J-H$ vs $H-K_s$ color-color diagram (see Section 4.2), (3) 196 known or candidate members of the Chamaeleon I molecular cloud identified prior to this study (see Appendix), (4) x-ray sources selected from the ROSAT all-sky survey (Alcalá et al. 1995), and (5) an image of the average $H-K_s$ color in the point source list binned to a resolution of $5'$. The overall density of stars increases from the south to the north, which reflects the decreasing distance (galactic latitude from $-18°$ to $-13°$) to the galactic plane. Obscuration from dust in the Chamaeleon I molecular cloud is clearly manifested in a sharp decrease in the J-band star counts near the center of the image and a corresponding increase in the average $H-K_s$ color.

Variable stars are found over the entire 6° long region with a clear enhancement toward 2 regions in the molecular cloud at declinations of $\sim -76.5°$ and $\sim -77.5°$. The declination band between $-76.2°$ and $-77.8°$ that encompasses these two regions contains 63% (60/95) of the total number of identified variable stars despite containing only 27% of the survey area. The fact that the variable star surface density is highest toward the molecular cloud where the overall stellar density is lowest suggests direct affiliation of the variable stars with the molecular cloud and hence a young stellar population. Indeed, 45 of the 95 variable stars have been previously identified as likely members of the Chamaeleon I T Tauri association. Of the remaining 50 objects, 15 are projected against the molecular cloud and are discussed as possible Chamaeleon I members in Section 4, and 35 are distributed over a larger region outside the molecular cloud boundaries. This widespread variable population may represent either variable field stars, intermediate age ($>$ 10 Myr) pre-main-sequence stars that have formed in the vicinity of the Chamaeleon I molecular cloud, or young ($<$ 10 Myr) pre-main-sequence stars formed in Chamaeleon I that have drifted from the molecular cloud. The data obtained here do not enable us to make a definitive interpretation of these variable stars, although as discussed in the following section, the colors and magnitudes of these stars suggest they are not likely to be a young stellar population related to the Chamaeleon I molecular cloud.

3.4. Colors and Magnitudes of the Variable Stars

The nature of the variable stars can be clarified by analyzing their colors and magnitudes. At the sensitivity of the 2MASS observations, the field star population is dominated by main sequence stars of spectral type late-F to early-K (see, e.g., Wainscoat et al. 1992). In contrast, most of the known members of Chamaeleon I have K and M spectral types (Lawson, Feigelson, & Huenemoerder 1996), and should have redder intrinsic colors than the field stars. Moreover, given the proximity and youth of the Chamaeleon I association, pre-main-sequence stars in Chamaeleon I will have brighter apparent magnitudes than the typical field star of the same spectral type.

To examine the colors and magnitudes for the stars detected in our observations, Figure 5 shows the K_s vs $H - K_s$ diagram for the variable star population (circles) compared to all sources detected in the survey (represented in Hess format by the color scale). The filled circles indicate the subset of variable stars that have been previously identified as members or candidate members of Chamaeleon I (see Appendix). The black solid line in Figure 5 shows the 2 Myr pre-main-sequence isochrone from D'Antona & Mazzitelli (1997,98), corresponding to the mean age of the cluster (Lawson, Feigelson, & Huenemoerder 1996), and the dashed line shows the interstellar reddening vector. The variables can be coarsely grouped into two populations: (1) bright ($K_s \lesssim 12$) and red ($H - K_s \gtrsim 0.3$) stars, and (2) relatively faint and blue stars. Most of the bright red variables are known members of Chamaeleon I with colors and magnitudes consistent with a young, reddened, pre-main-sequence population. Further, as shown in Figure 6, many of these red variables exhibit a near-infrared excess in the $J - H$ vs. $H - K_s$ color-color diagram consistent with the presence of an optically thick circumstellar accretion disk (Lada & Adams 1992; Meyer, Calvet, & Hillenbrand 1997).

To further investigate the distinction between "red" and "blue" variable stars, Figure 7 shows the spatial distribution of variables separated by $H - K_s$ color, where the filled symbols again represent previously known Chamaeleon I members. Not surprisingly most of the red variable stars are found toward the Chamaeleon I molecular cloud and suggest that the red colors can be attributed to a combination of extinction, near-infrared excess emission, and late spectral types for many of the association members. Four stars with red colors are found outside the boundaries of the Chamaeleon I molecular cloud. One of these variable stars is XZ Cha, thought to be a Mira star. A second is a suggested optical counterpart to a ROSAT x-ray source RX J1108.8-7919b, and is likely a pre-main-sequence star (Alcalá et al. 1995). A third red variable is PU Car[2], a variable star of unknown type. The fourth red variable located off of the Chamaeleon I molecular cloud is anonymous.

In contrast to the red variable stars, the blue variables are found scattered over the entire 6° declination range of the survey. Figure 5 shows that in general these stars are too blue to be consistent with the 2 Myr old Chamaeleon I pre-main-sequence population. The blue variable stars may represent either field stars unrelated to Chamaeleon I, or older pre-main-sequence stars that have formed in Chamaeleon I or its vicinity, but have since dispersed around the cloud. For example, assuming a $1\,\mathrm{km\,s^{-1}}$ velocity dispersion, a 10 Myr pre-main-sequence population at the distance of Chamaeleon I will disperse over a 3° radius region if the binding energy from the molecular cloud is negligible. We find near-infrared variables over at least 6° centered on Chamaeleon I.

To investigate whether the faint, blue variable stars could plausibly represent an older generation of stars in the vicinity of the Chamaeleon I molecular cloud, the green dotted curve in Figure 5 shows the 10 Myr pre-main-sequence isochrone. As stars and brown dwarfs evolve toward

[2]Alcalá et al. (1995) identified PU Car as RX J1108.8-7519b. However, based on the finding charts from Hoffmeister (1963), PU Car is located 2.5′ south of this x-ray source.

the main-sequence, they become blue and fainter, but even compared to the 10 Myr old isochrone, most of faint variable stars have colors that are too blue. While it is unlikely that the widely distribution variables are comprised of low mass stars < 10 Myr old, their colors and magnitudes are consistent with an older population (> 10 Myr) of low mass pre-main-sequence stars ($< 1M_{\odot}$) located beyond the Chamaeleon I cloud. Such a population could have formed at the edge of an H I spur associated with Upper Sco OB association, similar to the eta Cha and TW Hya associations (Mamajek & Feigelson 2001).

Alternatively, the blue variables have properties roughly expected from a main-sequence field star population in that they coincide with the peak density of field stars shown in Figure 5, exhibit a north-south gradient in their spatial distribution (see Figs. 5 and 7), and have colors consistent with G- and K-dwarfs (see Fig. 6). The main difficulty with this interpretation is in understanding the origin of the near-infrared variability if these are indeed old field stars. Follow-up spectroscopic observations to search for lithium in these sources will help distinguish if the widespread variable stars are field objects or a > 10 Myr pre-main-sequence population.

4. Candidate Members of the Chamaeleon I Molecular Cloud

As summarized in the Appendix, the current census of the stellar population in the Chamaeleon I molecular cloud has been established based on optical variability studies, optical spectroscopy, x-rays, and infrared surveys. The monitoring observations obtained here complement and expand these previous studies, and allow candidate members to be identified based on variability in the J, H, and K_s time-series data and from near-infrared excesses in the $J - H$ vs. $H - K_s$ color-color diagram. In this section, we use our infrared variability data to identify new candidate members of the Chamaeleon I association and comment on the completeness of the current stellar/substellar membership.

4.1. Variables

Of the 95 variable stars identified in the survey, 45 are associated with stars that have been suggested previously as members of Chamaeleon I. As discussed in Section 3.4, most of the remaining 50 variable stars are likely field stars or an intermediate age ($\gtrsim 10$ Myr) pre-main-sequence population based on their colors, magnitudes, and spatial distribution. However, 5 variable stars have near-infrared colors ($H - K_s > 0.3$) and coordinates ($-77.8^{\circ} < \delta < -76.2^{\circ}$) generally consistent with being cluster members (see Fig. 7). Of these 5 stars, one is YY Cha with a magnitude of $K_s = 4.891$, and is most likely a Mira variable (Whittet, Prusti, & Wesselius 1991). The remaining four stars have not been previously identified as variable stars; their ID numbers, coordinates, and photometry are summarized in Table 4. The K_s-band magnitudes range of these 4 variables range from 10.8 to 13.5, and two objects (9484 and 15991) have K_s magnitudes and $H - K_s$ colors that

imply masses below the hydrogen burning limit if they are 2 Myr old objects at the distance of Chamaeleon I. As described in the next section, two of these variable stars (1715 and 15991) also exhibit an apparent near-infrared excess in the $J-H$ vs. $H-K_s$ color-color diagram, which provides additional evidence that they are likely members of the Chamaeleon I association.

4.2. Near-infrared Excess

Previous studies have identified candidate members of Chamaeleon I based on the presence of a near-infrared excess in a color-color diagram (Cambrésy et al. 1998; Oasa, Tamura, & Sugitani 1999; Gómez & Kenyon 2001). The angular extent of our survey and the precision that results from averaging all of the photometric measurements (typically between 12 and 25 independent observations per band per star) has produced an extensive, high signal-to-noise database of near-infrared photometry with which to conduct a more accurate census of stars with near-infrared excesses than previously possible. For the purpose of this exercise, a star was defined to have a near-infrared excess if the average colors of all photometric measurements are such that the star is located to the right of the rightmost reddening vector shown in Figure 6. This approach is sensitive to stars with large enough infrared excesses to shift the observed colors outside the reddening vector drawn from the extrema of the color range at early O and late M spectral types. Stars with smaller infrared excess cannot be distinguished from reddened field stars in this diagram. The main-sequence locus and reddening vector were adopted from Bessell & Brett (1988) and Cohen et al. (1981) respectively, and transformed into the 2MASS photometric system using the relations in Carpenter (2001). The main-sequence locus from Bessell & Brett (1988) extends to M6 spectral types. Therefore, stars located to the right of the reddening vector may signify an apparent infrared excess due to photometric noise, a true infrared excess presumably due to an optically thick inner circumstellar disk, or a spectral type later than M6 but earlier than $\sim$L9 (Kirkpatrick et al. 2000; Leggett et al. 2002), as the T-dwarfs have bluer infrared colors.

Figure 8 shows $J-H$ vs. $H-K$ color-color diagrams in 4 different K_s-band magnitude intervals for sources with at least 10 $J-H$ and $H-K_s$ measurements. The later criteria was arbitrarily imposed to ensure high signal-to-noise photometry. Sources brighter than K_s=14 and with near-infrared excess have $J-H$ colors that range between $\sim$1 and 3 mag. Spatially these bright sources are located toward the Chamaeleon I molecular cloud (see Fig. 4). These properties are consistent with the notion that the bright objects with infrared excesses are pre-main-sequence stars surrounded by optically thick accretion disks embedded within the Chamaeleon I molecular cloud.

The K_s vs. $H-K_s$ color-magnitude diagram for the 208 sources with an apparent near-infrared excess is shown in Figure 9, where filled symbols denote stars with a near-infrared excess that also show infrared variability, and open symbols indicate non-variable sources with an excess. Figure 9 shows that all but one source with a near-infrared excess and brighter than K_s=11.5 (approximately the hydrogen burning limit for the distance and age of Chamaeleon I with no extinction) is also

variable in the near-infrared. The one star (ID number 1959) with an apparent infrared excess and is not variable has blue infrared colors ($J-H$,$H-K_s$ = 0.104, 0.120) and possesses a small near-infrared excess. The $H-K_s$ color for this star is too blue to be consistent with membership in the Chamaeleon I association assuming an age of 2 Myr. We suspect therefore that this star most likely has an apparent near-infrared excess due to photometric noise, and we do not list this star as a candidate member of Chamaeleon I.

Figures 8 and 9 also show a population of 155 sources fainter than $K_s = 14$ that, if stellar, exhibit a near-infrared excess. From visual inspection of the images, a few of these sources have suspect photometry due to a nearby bright star or a close companion. However, for most of the objects, there is no a priori reason to question the photometry. The apparent excesses cannot be attributed to random photometric noise since one would expect that these objects would be present with colors ranging from $J-H = 0.3$ to 0.9 where the stellar density is highest in the color-color plot. Instead, most of the faint objects with excesses are found in a narrow range of colors between $J-H = 0.8$ and 1.0. Spatially these objects are found over the full 6° declination range of the survey. While we cannot exclude the possibility that these objects are very low mass objects dispersed from Chamaeleon I, such a scenario would seem unlikely since it would require disparate spatial distributions between the substellar and the stellar populations, and would imply that the Chamaeleon I IMF is heavily weighted toward brown dwarf objects in contrast to the IMF in other nearby star forming regions (see, e.g., Luhman et al. 2000). The faint infrared excess objects cannot be field brown dwarfs since their surface density of $\sim$15 deg^{-2} between $K_s = 14$ and 14.5 is $\sim$300 times larger than the surface density of L-dwarfs down to $K_s = 14.5$ (Kirkpatrick et al. 1999).

The remaining possibility then is that the faint sources with near-infrared excesses are galaxies, where the recessional velocities shift the galaxy colors to the right of the reddening vector in the $J-H$ vs. $H-K_s$ diagram. The near-infrared colors observed in Figure 8 can be accounted for by a population of galaxies at redshifts between $\sim$0.1 and 0.25 (Mannucci et al. 2001). Photometric and spectroscopic surveys have in fact shown that galaxies with magnitudes of K=14-15 have a mean redshift of 0.18 (Songaila et al. 1994) and a surface density of $\sim$100 deg^{-2} (Väisänen et al. 2000). By comparison, the observed surface density of sources in Chamaeleon I with near-infrared excesses and fainter than K_s=14 is $\sim$35 deg^{-2}. The lower surface density of faint near-infrared excess sources compared to the expected galaxy population may be attributed to the high extinction from the Chamaeleon I molecular cloud and that not all of the galaxies will have high enough redshift to produce the red near-infrared colors. We therefore conclude that the sources with a near-infrared excess and fainter than K_s=14 consist predominantly of galaxies with redshifts of $\sim$0.2.

Given the apparent predominance of galaxies among the near-infrared excess objects at faint magnitudes, we only considered infrared excess sources brighter than K_s =13.5 as possible members of Chamaeleon I. The spatial distribution of these 45 objects is shown in the third panel of Figure 4. All but one is concentrated toward the cloud. The one exception, star 11564 in our source list (J2000 equatorial coordinates of α, δ = 11:08:03.56,−79:22:34.65), has average colors of $J-H$=0.976 and

$H-K_s$=1.218. The infrared excess appears in each of the 24 individual photometric measurements with a PSF chi-square less than 2 in all observations. Therefore, the near-infrared excess cannot be merely due to photometric noise or a poor PSF fit. This object may either be an isolated young star with near-infrared excess, or a bright, red galaxy. We interpret the remainder of the near-infrared excess sources brighter than K_s=13.5 as young stellar objects whose excesses can be accounted for by an optically thick inner circumstellar disk for the brighter objects, and/or a spectral type later than $\sim$M6 for the fainter objects. Table 4 lists the seven new near-infrared candidates members identified from our observations that are located in the vicinity of the Chamaeleon I molecular cloud. (The eight star with an infrared excess in Table 4 is fainter than our imposed magnitude limit, but is included in the table as a candidate members because it is a variable.)

We note that we did not confirm many of the near-infrared excess stars identified in previous studies. Cambrésy et al. (1998) selected 54 candidate members in Chamaeleon I based on near-infrared excess in the $I-J$ vs. $J-K$ diagram or redder colors than expected from a Chamaeleon I extinction map. Of these 54 stars, 42 are in our database with three-band photometry, and only 6 show an infrared excess in our data. One of these sources is identified in Table 4, and three others (ID numbers 32, 41, and 49 in Table 2 of Cambresy et al. 1998) are indicated as candidate members in the Appendix since they have other characteristics that suggest they may be pre-main-sequence stars. The remaining two sources (ID numbers 329 and 926 in our study, and ID 10 and 11 respectively in Cambresy et al. 1998) show infrared excess in our data as well, but they were detected on only 5-6 J-band images due to the faintness of the object and were not included in the near-infrared excess analysis. Similarly, Gómez & Kenyon (2001) list 56 infrared excess candidates (identified from the $J-H$ vs. $H-K_s$ diagram) brighter than K_s=14, of which 49 are three band detections in our observations. Only 7 of these sources show an infrared excess. One of these objects is indicated in Table 4, four others (ID numbers 13, 29, 30, and 31 in Gomez & Kenyon 2001) are listed in the Appendix as members based on other studies, and 2 (ID numbers 10 and 40 in Gomez & Kenyon 2001) are fainter than K_s =14 in our study and did not meet our magnitude criterion. (As shown in CHS01, some stars do show a transient near-infrared excess. However, it is unlikely that this account can account for the majority of the Gomez & Kenyon sources since an equally large number of new near-infrared excesses should have been identified in our observations, which is not observed.) Finally, Oasa, Tamura, & Sugitani (1999) list 19 sources with infrared excesses, of which 12 are in our database. The remaining 7 sources are fainter than our sensitivity limits. Of these 12 sources, 7 show an infrared excess. All of the infrared excess candidates from Oasa, Tamura, & Sugitani (1999) are listed in the Appendix.

4.3. Discussion

The area covered by our observations encompasses 170 known or candidate Chamaeleon I members identified prior to this study, of which 159 have been detected in the near-infrared with our data. As discussed in CHS01, the monitoring observations discussed here are most sensitive to

detecting variables brighter than $K_s \sim 12$. Of the 129 Chamaeleon I members brighter than this limit, 43, or 33%, have been detected as variable. The variables include stars with and without near-infrared excesses as traced in the $J-H$ vs. $H-K_s$ diagram, although the variability observations are biased toward detecting stars with excesses. That is, of the Chamaeleon I members brighter than K_s=12, 23% (30/129) have a near-infrared excess, but 28/43 (65%) of the variables have an excess. Thus the proportion of bright stars that have a near-infrared excess is higher among the variable compared to the Chamaeleon I members at a $\sim 5\sigma$ confidence level. Similarly, in Orion, 19%±1% of the stars brighter than K_s=12 exhibit a near-infrared excess, compared to 28%±2% of the variables brighter than this limit. While the Orion variables are also slightly biased toward stars with infrared excesses (at the $\sim 4.5\sigma$ confidence level), the bias is not as strong in that the overall percentage of variables with an infrared excess is lower in Orion by a factor of 2.3±0.3.

The fact that nearly all Chamaeleon I members with a near-infrared excess and brighter than K_s=12 are also variable suggests that the variability may be related to the presence of an inner accretion disk. Further evidence for this conjecture comes from the type of variability exhibited by stars with infrared excesses. Of the 14 stars in Chamaeleon I that show measurable color variability where the stellar color becomes redder as the star fades (see Section 3.2), 12 have a near-infrared excess. These near-infrared color variations cannot be readily accounted for by cool spots on the stellar surface (Skrutskie et al. 1996; CHS01). They can however, be explained by extinction variations (perhaps from a warped circumstellar disk), or hot spots on the stellar surface produced by accretion from the disk onto the star. However, hot spots can only produce colors variations of up to ~ 0.1 mag in the near-infrared given typical hot spot parameters modeled in T Tauri stars, and extinction variations may be the preferred explanation for the large amplitude variables (see CHS01). More extensive observations and modeling of these color variations may provide a unique window into the properties of the inner circumstellar disk.

Two of the Chamaeleon I variables (ID numbers 18416 and 21473) that show color variations have masses near the hydrogen burning limit as inferred from the K_s vs. $H-K_s$ diagram. This suggests that the variability mechanisms discussed in context of the Orion observations for stars more massive than $1\,\mathrm{M}_\odot$ may extend to lower mass objects. For fainter sources between K_s magnitudes of 12.0 to 13.5, and presumably lower mass, only 8% (1/13) of the near-infrared excess objects also show variability. The lack of variability in these sources does not necessarily imply a change in the infrared excess-variability relation for substellar objects however. Not only are these observations less sensitive to variability for sources fainter than K_s=12, but the apparent infrared excess may be due to a spectral type later than M6 and not to a circumstellar disk.

Finally, we briefly discuss the implication of these observations for the current census of the stellar and substellar population in Chamaeleon I. The region we surveyed contains 129 known or candidate Chamaeleon I members brighter than K_s=12. Only 2 new candidate members brighter than $K_s = 12$ have been identified in this study from either variability or a near-infrared excess. Since nearly all bright objects with a near-infrared excess are also variable, these observations suggest that the current census of Chamaeleon I sources is nearly complete for objects brighter

than K_s=12 and with an infrared excess in the $J-H$ vs. $H-K_s$ diagram. Comerón, Neuhäuser, & Kaas (2000) recently identified 13 low mass stars and brown dwarfs in Chamaeleon I from an Hα prism survey. Nine of these sources have magnitudes of $10.6 < K_s < 12$, but none were detected as variable, and only one was identified as distinctive in this dataset because of an apparent infrared excess. The other 4 sources in Comerón, Neuhäuser, & Kaas (2000) are fainter than K_s=12, and interestingly, 3 were identified here as having a near-infrared excess, where the excess for these objects may be due to a late spectral type. While the statistics are small, the comparison with Comerón, Neuhäuser, & Kaas (2000) suggests that the $J-H$ vs. $H-K_s$ diagram is fairly efficient at identifying the substellar objects. The fact that only 8 new candidate members were identified with magnitudes of $12 < K_s < 13.5$ suggests brown dwarfs will not substantially expand the current population census of Chamaeleon I.

5. Summary

We have conducted a J, H, and K_s variability study of stars in a $0.72^\circ \times 6^\circ$ region centered on the Chamaeleon I molecular cloud and T-association. Observations were obtained on 2 nights in January 2000 and 13 nights in April and May 2000 using the 2MASS South telescope. Compared to our variability study of the Orion A molecular cloud (CHS01), which was sensitive to variable stars more massive than $\sim 1\,\mathrm{M}_\odot$, observations of the closer Chamaeleon I star forming region permit variability to be detected in lower mass stars and brown dwarfs down to $\sim 0.05\,\mathrm{M}_\odot$.

Of the 34,539 sources meeting the photometric completeness criteria, 95 have been identified as variable from either a large Stetson (1996) variability index or a large reduced chi-square in the time series data. The variables can be coarsely grouped into a population of bright ($K_s < 12$), red ($H-K_s > 0.3$) stars and a population of faint ($K_s < 13$), blue ($H-K_s < 0.3$) stars. Most of the "red" variables are known members of the Chamaeleon I association, and as expected have near-infrared colors and magnitudes consistent with a young, pre-main-sequence population. The "blue" variables are distributed over the full 6° of the survey area. The colors and magnitudes of the blue variables are inconsistent with a pre-main-sequence population as old as 10 Myr at the distance of Chamaeleon I, but can be explained as a population of older pre-main-sequence stars unrelated to Chamaeleon I or variable field stars.

The time-series data were used to identify new candidate members of the Chamaeleon I association that show photometric variability and/or a near-infrared excess characteristics of an optically thick circumstellar disk. Of the 95 variables identified in this study, 45 were known prior to this study as members or candidate members of Chamaeleon I. Among the remaining 50 variables, we have identified 4 new sources that have colors and coordinates consistent with low mass, pre-main-sequence members of the Chamaeleon I association. A total of 208 sources brighter than K_s=14.8 were identified as having a near-infrared excess in the $J-H$ vs. $H-K_s$ color-color diagram. The fainter sources with near-infrared excesses ($K_s < 14$) are randomly distributed over the 6° survey region. Based on their spatial distribution, location in the color-color diagram, and surface density,

we suggest that these objects are most likely galaxies with redshifts of $z \lesssim 0.25$. The 45 sources brighter than K_s=14.5 and with infrared excesses are clustered spatially around the Chamaeleon I molecular cloud and are likely association members. Seven of these relatively bright sources with excesses are new candidate members of Chamaeleon I, including one which is also variable. In total, 10 new candidate members have been identified, 8 of which have colors and magnitudes consistent with young brown dwarfs at the distance of Chamaeleon I. These observations suggest that the current census of the Chamaeleon I population is complete for objects brighter than K_s=12 and with a near-infrared excess in the $J - H$ vs. $H - K_s$ diagram.

As a product of this study, these observations have yielded a precise dataset of photometry and astrometry for previously identified Chamaeleon I members. In the Appendix we summarize the J, H, and K_s magnitudes and cross-identifications for Chamaeleon I members.

We would like to thank the 2MASS Observatory Staff and the Data Management Team for acquiring and pipeline processing the special survey observations used in this investigation. This publication makes use of data products from the Two Micron All Sky Survey, which is a joint project of the University of Massachusetts and the Infrared Processing and Analysis Center, funded by the National Aeronautics and Space Administration and the National Science Foundation. 2MASS science data and information services were provided by the InfraRed Science Archive (IRSA) at IPAC. This research has made use of the SIMBAD database, operated at CDS, Strasbourg, France. JMC acknowledges support from Long Term Space Astrophysics Grant NAG5-8217 and the Owens Valley Radio Observatory, which is supported by the National Science Foundation through grant AST-9981546.

A. Astrometry and Photometry for Previously Identified Members of Chamaeleon I

During the course of this study, a membership list for Chamaeleon I was compiled using published observations. This Appendix presents the compilation of known and candidate members of the Chamaeleon I association, and summarizes the astrometry and J, H, and K_s photometry obtained from our observations.

The Chamaeleon I association was initially identified as a spatial concentration of optical variable stars (Hoffmeister 1962). Subsequent studies expanded the association membership through objective prism or CCD Hα emission-line surveys (Henize & Mendoza 1973; Schwartz 1977; Hartigan 1993) and spectroscopic follow-up of individual stars (Appenzeller 1977,79; Rydgren 1980; Appenzeller, Jankovics, & Krautter 1983) to identify stars with spectral features characteristic of pre-main-sequence objects. More recent objective prism surveys, followed by spectroscopic observations and multi-wavelength imaging, have begun to probe the Chamaeleon I population in the substellar regime (Comerón, Rieke, & Neuhäuser 1999; Comerón, Neuhäuser, & Kaas 2000). Additional pre-main-sequence candidates have been identified in x-rays from Einstein (Feigelson & Kriss 1989) and ROSAT (Feigelson et al. 1993; Alcalá et al. 1995), where pre-main-sequence counterparts to the x-ray sources have been identified from optical spectroscopic follow-up observations (Walter 1992; Huenemoerder, Lawson, & Feigelson 1994; Alcalá et al. 1995; Lawson, Feigelson, & Huenemoerder 1996). Candidate cloud members that remain deeply embedded in the cloud have been identified from the presence of excess near-infrared emission (Hyland, Jones, & Mitchell 1982; Jones et al. 1985; Cambrésy et al. 1998; Oasa, Tamura, & Sugitani 1999; Gómez & Kenyon 2001), red far-infrared colors from IRAS (Baud et al. 1984; Assendorp et al. 1990; Prusti et al. 1991; Whittet, Prusti, & Wesselius 1991; Gauvin & Strom 1992), and more recently, red mid-infrared colors from ISO (Nordh et al. 1996; Persi et al. 2000; Lehtinen et al. 2001). In total, the candidate members identified by infrared excesses can more than double the known stellar population.

Table 5 summarizes the status of the stellar and substellar membership in the Chamaeleon I molecular cloud prior to this study. We include in Table 5 stars that are optically variable or show Hα emission as summarized by Whittet et al. (1987) and references therein for pre-1987 observations, the Hα objects and red stars from Hartigan (1993), the brown dwarfs from Comerón, Neuhäuser, & Kaas (2000), candidate members identified from IRAS (Baud et al. 1984; Whittet, Prusti, & Wesselius 1991) and ISO (Persi et al. 2000), and optical counterparts to x-ray sources that have spectroscopic signatures of pre-main-sequence stars (Walter 1992; Lawson, Feigelson, & Huenemoerder 1996). Table 5 also included possible deeply embedded members of Chamaeleon I that have recently been identified by the presence of excessed near-infrared (Oasa, Tamura, & Sugitani 1999) and mid-infrared emission (Persi et al. 2000). Cambrésy et al. (1998) and Gómez & Kenyon (2001) have also identified $\sim$150 candidate members based on the presence of near-infrared excess emission (and, in the case Cambresy et al. 1998, red sources without necessarily an infrared excess). Since the majority of the near-infrared excess candidates could not be confirmed with our data (see Section 4.2), these objects are not listed in Table 5 unless that stars contains other characteristics indicating it is a pre-main-sequence object (see also Table 4).

Column 1 in Table 5 lists the commonly adopted name of the Chamaeleon I members. Due to the multitude of observations of the Chamaeleon I region, many of the sources have been observed as part of several studies, and the cross identifications of the various names are provided in Table 6. Most of the cross identifications were made by matching the coordinates in the original references. Two notable exceptions are that the positions for sources in the General Catalog of Variable stars were taken from López & Girard (1990) when possible, and the association of IRAS sources from Baud et al. (1984) were taken from Lawson, Feigelson, & Huenemoerder (1996). Columns 2 and 3 list the J2000 equatorial coordinates, where the coordinates have been obtained from, in order of preference, (1) this study, (2) the 2MASS Working Database (Version 2 processing) for stars outside our survey coverage, and (3) the literature. The coordinates listed in Oasa, Tamura, & Sugitani (1999) were found to differ from 2MASS by up to $10''$. For sources detected only by Oasa, Tamura, & Sugitani (1999), an astrometric correction was applied based on nearby sources detected both by our observations and Oasa, Tamura, & Sugitani (1999). Columns 4-12 list the mean J, H, and K_s magnitudes, photometric RMS, and number of measurements. Column 13 lists the Stetson variability index derived from our data. 2MASS photometry for Chamaeleon I members located outside our survey boundaries have been obtained from the Version 2 2MASS Working Database. These sources can be identified in Table 5 as having no Stetson index and with N$\leq$=1 in each band. The RMS in such instances represent the photometric uncertainty from the 2MASS data reduction pipeline excluding zero point calibration uncertainties, which are typically $\sim$1% in each band.

As noted by Schwartz (1991), many of the sources are only suspected members of the cloud and have yet to be verified spectroscopically to be pre-main-sequence stars. In particular, some stars have been identified as Chamaeleon I members because they are variable or have red photometric colors (but without an infrared excess), but no additional evidence has been obtained to indicate these are not simply field stars. Accordingly, the flags in Column 11 indicate the properties associated with each source that suggests it is a pre-main-sequence object. The flags indicate, in order from left to right, (1) known variables from the General Catalog of Variable Stars or this study; (2) Hα emitting objects from Henize & Mendoza (1973), Schwartz (1977); Hartigan (1993), Walter (1992), Huenemoerder, Lawson, & Feigelson (1994), Lawson, Feigelson, & Huenemoerder (1996), Comerón, Rieke, & Neuhäuser (1999), and Comerón, Neuhäuser, & Kaas (2000), and objects with Paβ or Brγ in emission from Gómez & Persi (2002); (3) stars with lithium in absorption from Walter (1992), Huenemoerder, Lawson, & Feigelson (1994), and Lawson, Feigelson, & Huenemoerder (1996); (4) x-ray sources from Feigelson & Kriss (1989) and Feigelson et al. (1993); (5) near- or mid-infrared excesses from Oasa, Tamura, & Sugitani (1999), Persi et al. (2000), and this study; and (6) far-infrared sources from Baud et al. (1984), Assendorp et al. (1990), Prusti et al. (1991), and *IRAS* Point Source Catalog. The flag 'Y' indicates the characteristic has been identified with that star in at least one study; The flag '?' indicates that the authors of the original paper expressed uncertainty of the detection; and the flag '0' indicates the property has not yet been identified.

Notes on individual sources:

UX Cha — Feigelson & Kriss (1989) associated UX Cha (= T 22) with the x-ray source CHX 8. However, as originally noted by Feigelson et al. (1993), UX Cha is actually located 26″ to the north. The finder chart in Schwartz (1991) identifies the incorrect star as UX Cha.

C9-1, C9-2, and C9-3 — Hyland, Jones, & Mitchell (1982) identified these objects as Chamaeleon I members based on bolometer data. Each of these objects is located in the bright Infrared Nebula (IRN). However, none of these sources are visible on the 2MASS images. While it is possible that these objects are variable and have faded from view, we find it more likely that they are knots in nebulosity and have not included these objects in the membership list.

T 2 — This source has been traditionally identified as a member of Chamaeleon I based on its optical variability. However, Winterberg & Bruch (1996) showed that this source is a RR Lyra star unrelated to Chamaeleon I. This source is not listed in Table 5.

T 36 — This source has traditionally been associated with Chamaeleon I based on its optical variability, but the near-infrared colors and magnitudes of this star (K_s=12.809, $H-K_s$=0.184 are inconsistent with membership. While this star is listed in Table 5, spectroscopic observations are needed to ascertain membership.

T49, CHX 18N, and IRAS 11101-7603 — The IRAS source is closest to CHX 18N, but within the IRAS astrometric uncertainties may also be associated with T 49. It is listed under both objects in Table 5.

T 52 and T 53 — Feigelson & Kriss (1989) lists both sources as possible optical counterparts to the x-ray source CHX 19. Subsequent high resolution observations with ROSAT show the x-ray emission originates from T 52. (Feigelson et al. 1993). Therefore, we have not listed T 53 as a counterpart to CHX 19 in Table 6.

CHXR 30 and B 38 — Lawson, Feigelson, & Huenemoerder (1996) associates CHXR 30 with B 38, while Cambrésy et al. (1998) and Kenyon, & Gómez (2001) list CHXR 30 and B 38 as separate sources. Two stars separated by 9.9″ are present on the 2MASS images. The eastern source is consistently identified as CHXR 30 in these studies. It is the brighter of the two 2MASS sources in the optical with a $J-K_s$ color of 2.70. This star has not been conclusively been identified as pre-main-sequence object through spectroscopy, although Persi et al. (2000) identified a mid-infrared excess in this source from ISO observations. The western source, identified as B38 (Baud et al. 1984) by Cambrésy et al. (1998) and Kenyon, & Gómez (2001), is the redder of the two 2MASS objects with $J-K_s$=3.45. This source is detected as a variable with a near-infrared excess in our observations. Since the beam of the IRAS observations used by Baud et al. (1984) encompasses both 2MASS sources, and the position uncertainty of the ROSAT x-ray observations is 8″, it is not clear which, or if both, sources contribute to the far-infrared and x-ray emission. In Table 5, we list the eastern source as CHXR 30a and B 38a, and the western source as CHXR30b and B 38b.

HM 8 and ISO 10 — Persi et al. (2000) tentatively matched ISO 10 with HM 8, but they noted the larger than average positional differences between the two objects. The positional difference is larger than the tolerance limit used here to match the ISO catalog with the 2MASS astrometry, and this association was not made in Table 5.

REFERENCES

Alcalá, J. M., Krautter, J., Schmitt, J. H. M. M., Covino, E., Wichmann, R., & Mundt, R. 1995, A&AS, 114, 109

Appenzeller, I. 1977, A&A, 61, 21

_____ . 1979, A&A, 71, 305

Appenzeller, I., Jankovics, I., & Krautter, J. 1983, A&AS, 53, 291

Assendorp, R., Wesselius, P. R., Whittet, D. C. B., & Prusti, T. 1990, MNRAS, 247, 624

Baud, B., Young, E., Beichman, C. A., Beintema, D. A., Emerson, J. P., Habing, H. J., Harris, S., Jennings, R. E., Marsden, P. L., & Wesselius, P. R. 1984, ApJ, 278, L53

Bessell, M. S., & Brett, J. M. 1988, PASP, 100, 1134

Cambrésy, L., Copet, E., Epchtein, N., de Batz, B., Borsenberger, J., Fouqué, P., Kimeswenger, S., & Tiphène, D. 1998, A&A, 338, 977

Carpenter, J. M. 2001, AJ, 121, 2851

Carpenter, J. M., Hillenbrand, L. A., & Skrutskie, M. F. 2001, AJ, 121, 3160 (CHS01)

Cohen, J. G., Grogel, J. A., Perrson, S. E., & Elias, J. H. 1981, ApJ, 249, 481

Comerón, F., Rieke, G. H., & Neuhäuser, R., 1999, A&A, 343, 477

Comerón, F., Neuhäuser, R., & Kaas, A. A. 2000, A&A, 359, 269

Cutri, R. M. et al. 2000, Explanatory Supplement to the 2MASS Second Incremental Data Release, http://www.ipac.caltech.edu/2mass/releases/second/doc/explsup.html

D'Antona, F., & Mazzitelli, I. 1997, Mem. Soc. Astron. Italiana, 68, 807

D'Antona, F., & Mazzitelli, I. 1998, ASP conf. ser. 134, "Brown Dwarfs and Extrasolar Planets", eds. R. Rebolo, E. L. Martin, and M. R. Zapatero-Osorio (San Franciso: ASP),442

Feigelson, E. D., Casanova, S., Montmerle, T., & Guibert, J. 1993, ApJ, 416, 623

Feigelson, E. D., & Kriss, G. A. 1989, ApJ, 338, 262

Gauvin, L. S., & Strom, K. M. 1992, ApJ, 385, 217

Gómez, M. & Kenyon, S. J. 2001, AJ, 121, 974

Gómez, M. & Persi, P. 2002, A&A, in press

Hartigan, P. 1993, AJ, 105, 1511

Henize, K. G., & Mendoza, E. E. 1973, ApJ, 180, 115

Hillenbrand, L. A., Strom, S. E., Calvet, N., Merrill, K., M., Gatley, I., Makidon, R. B., Meyer, M. R., & Skrutskie, M. F. 1998, AJ, 116, 1816

Hoffmeister, C. 1962, Zs. f. Ap. 55, 290

_____ 1963, Veröff. Sternw. Sonneberg, 6, 1

Huenemoerder, D. P., Lawson, W. A., & Feigelson, E. D., 1994, MNRAS, 271, 967

Hyland, A. R., Jones, T. J., & Mitchell, R. M. 1982, MNRAS, 201, 1095

Jones, T. J., Hyland, A. R., Harvey, P. M., Wilking, B. A., & Joy, M. 1985, AJ, 90, 1191

Kenyon, S. J., & Gómez, M. 2001, AJ, 121, 2673

Kirkpatrick, D. J. et al. 1999, ApJ, 519, 802

Kirkpatrick, D. J. et al. 2000, AJ, 120, 447

Lada, C. J, & Adams, F. C. 1992, ApJ, 393, 278

Lawson, W. A., Feigelson, E. D., & Huenemoerder, D. P. 1996, MNRAS, 280, 1071

Leggett, S. K., et al. 2002, ApJ, 564, 452

Lehtinen, K., Haikala, L. K., Mattila, K., & Lemke, D. 2001, A&A, 367, 311

López, C. E. & Girard, T. M. 1990, PASP, 102, 1018

Luhman, K. L., Rieke, G. H., Young, E. T., Cotera, A. S., Chen, H., Rieke, M. J., Schneider, G., & Thompson, R. I. 2000, ApJ, 540, 1016

Mamajek, E. E. & Feigelson, E. D. 2001, Young Stars Near Earth: Progress and Prospects, ASP Conference Series Vol. 244. ed. R. Jayawardhana and T. Greene. (San Francisco: Astronomical Society of the Pacific)

Mannucci, F., Basile, F., Poggianti, B., Cimatti, A., Daddi, E., Pozzetti, L., & Vanzi, L. 2001, MNRAS, 326, 745

Meyer, M. R., Calvet, N., & Hillenbrand, L. A. 1997, AJ, 114, 288

Oasa, Y., Tamaura, M., & Sugitani, K. 1999, ApJ, 526, 336

Nordh, L. et al. 1996, A&A, 315, L175

Palla, F., & Stahler, S. W. 2000, ApJ, 540, 255

Persi, P. et al. 2000, A&A, 357, 219

Prusti, T., Clark, F. O., Whittet, D. C. B., Laureijs, R. J., & Zhang, C. Y. 1991, MNRAS, 251, 303

Rydgren, A. E. 1980, AJ, 85, 444

Schwartz, R. D. 1977, ApJS, 35, 161

_____ . 1991, in Low-Mass Star Formation in Southern Molecular Clouds, ed. B. Reipurth, ESO Sci. Rep., 11, 93

Skrutskie, M. F., Meyer, M. R., Whalen, D., & Hamilton, C. 1996, AJ, 112, 2168

Songaila, A., Cowie, L. L., Hu, E. M., & Gardner, J. P. 1994, ApJS, 94, 461

Stetson, P. B. 1996, PASP, 108, 851

Väisänen , P., Tollestrup, E. V., Willner, S. P. & Cohen, M. 2000, ApJ, 540, 593

Wainscoat, R. J., Cohen, M., Volk, K., Walker, H. J., & Schwartz, D. E. 1992, ApJS, 83, 111

Walter, F. M. 1992, AJ, 104, 758

Whittet, D. C. B., Kirrane, T. M., Kilkenny, D., Oates, A. P., Watson, F. G., & King, D. J. 1987, MNRAS, 224, 497

Whittet, D. C. B., Prusti, T., Franco, G. A. P., Gerakines, P. A., Kilkenny, D., Larson, K. A., & Wesselius, P. R. 1997, A&A, 327, 1194

Whittet, D. C. B., Prusti, T., & Wesselius, P. R. 1991, MNRAS, 249, 319

Winterberg, J., & Bruch, A. 1006, IAU Information Bulletin of Variable Stars, 4334

This preprint was prepared with the AAS LaTeX macros v5.0.

Table 1. Coordinates of Observed Tiles

Tile	Right Ascension[a]	Number of Nights Observed	
	(J2000)	Complete	Partial
1	$11^{h}04^{m}38^{s}$	18	3
2	$11^{h}06^{m}15^{s}$	22	3
3	$11^{h}07^{m}46^{s}$	26	3
4	$11^{h}09^{m}23^{s}$	28	3
5	$11^{h}10^{m}55^{s}$	26	3
6	$11^{h}12^{m}31^{s}$	21	3
7	$11^{h}14^{m}02^{s}$	16	3
8	$11^{h}15^{m}39^{s}$	16	3

[a]Each tile is $8.5' \times 6^{\circ}$ in size, and is centered on a declination of -77° and the right ascension listed.

Table 2. Observing Log

UT Date	Tile 8	Tile 7	Tile 6	Tile 5	Tile 4	Tile 3	Tile 2	Tile 1	Comments
January 13, 2000	x	x	x	x	x	x	x	x	$\delta < -78°$ only
January 25, 2000	x	x	x	x	x	x	x	x	$\delta > -78°$ only
April 8, 2000	x		x	x	x	x	x	x	
April 12, 2000	x	x	x	x	x	x	x	x	
April 19, 2000					x	x	x	x	
April 21, 2000	x	x	x	x	x	x	x	x	
April 22, 2000	x	x	x	x	x	x	x	x	
April 23, 2000	x	x	x	x	x	x	x	x	
April 24, 2000	x	x	x	x	x	x	x	x	
April 25, 2000	x	x	x	x	x	x	x	x	
April 27, 2000	x	x	x		x				
April 29, 2000	x	x	x	x	x	x	x	x	
May 1, 2000	x	x	x	x	x	x	x	x	
May 12, 2000	x	x	x	x					
May 19, 2000	x	x	x	x	x	x	x	x	

Table 3. Near-Infrared Variable Stars

ID	Name	Coordinates (J2000)		Mean Magnitudes			Observed RMS			N			Variability
		α	δ	J	H	K_s	J	H	K_s	J	H	K_s	Index
198	...	165.860056	−78.387932	13.805	13.361	13.174	0.140	0.131	0.113	12	12	12	3.03
241	...	165.868449	−77.457493	13.889	13.254	12.988	0.094	0.080	0.076	13	13	13	1.64
670	...	165.915725	−76.944871	14.014	13.605	13.489	0.131	0.148	0.134	13	13	13	2.85
776	...	165.925563	−75.089402	13.678	13.078	12.898	0.053	0.053	0.060	13	13	13	1.27
1012	Hn 2	165.948566	−77.332334	11.353	10.449	10.044	0.044	0.051	0.048	13	13	13	1.27
1715	...	166.017772	−76.659153	12.906	11.651	10.837	0.203	0.161	0.129	13	13	13	4.53
1898	T 14	166.037953	−76.455369	9.668	8.935	8.563	0.056	0.063	0.067	13	13	13	1.47
2168	...	166.062871	−76.110506	14.640	14.091	13.932	0.117	0.107	0.096	12	12	12	1.20
2225	...	166.068693	−76.469829	14.765	14.219	14.030	0.110	0.105	0.115	12	12	12	1.09
2745	...	166.122675	−76.938716	14.476	13.858	13.641	0.113	0.129	0.096	12	12	12	1.19
3131	...	166.161129	−74.019330	14.877	14.101	13.909	0.135	0.169	0.183	12	12	12	1.55
3616	...	166.207272	−75.686611	11.458	11.052	10.938	0.066	0.059	0.063	12	12	11	1.81
3841	...	166.234284	−74.561691	15.034	14.683	14.575	0.140	0.134	0.159	12	12	12	0.87
3876	T 16	166.237490	−77.265824	12.245	10.974	10.498	0.448	0.296	0.359	16	16	17	7.83
4862	...	166.330871	−76.140610	14.069	13.597	13.470	0.101	0.097	0.096	24	24	24	0.78
6771	...	166.520456	−78.550732	11.862	11.495	11.380	0.061	0.057	0.066	13	13	13	1.34
8073	...	166.657725	−79.169620	12.924	12.417	12.273	0.071	0.098	0.079	24	24	24	1.25
8234	Hn 5	166.674016	−76.596987	11.588	10.727	10.177	0.072	0.059	0.039	24	24	24	1.19
8369	CHXR 20	166.687729	−77.450689	10.717	9.628	9.134	0.617	0.458	0.334	24	24	24	12.42
8978	T 23	166.745878	−77.314854	11.195	10.429	9.999	0.044	0.051	0.049	24	23	23	1.20
9226	...	166.771953	−74.935493	13.841	13.521	13.421	0.146	0.162	0.147	24	24	24	3.49
9464	...	166.796780	−76.329690	13.696	13.180	13.037	0.192	0.185	0.172	24	24	24	3.54
9484	...	166.799142	−76.430582	13.667	12.904	12.466	0.066	0.054	0.041	24	24	24	0.62
9496	T 24	166.800185	−76.539810	10.829	9.837	9.325	0.170	0.145	0.088	24	24	22	3.63
9652	ISO 97	166.817455	−77.385247	...	13.841	11.451	...	0.134	0.102	0	24	24	1.58
9847	T 26	166.836317	−77.635363	7.810	6.941	6.224	0.021	0.034	0.040	23	23	23	0.74
10193	...	166.874272	−77.417151	12.163	11.353	10.958	0.121	0.112	0.111	17	19	16	3.12
10722	...	166.930706	−74.617254	13.937	13.525	13.412	0.072	0.041	0.056	12	12	12	0.33
10737	T 28	166.931849	−77.661457	10.196	9.013	8.304	0.043	0.049	0.058	11	11	10	1.20
10937	...	166.950921	−75.989196	13.953	13.480	13.398	0.070	0.054	0.048	12	12	12	0.59
11188	...	166.975914	−73.965912	15.444	14.670	14.559	0.149	0.167	0.165	12	12	12	0.48
11315	CHXR 30b	166.988649	−77.290661	13.278	11.119	9.825	0.204	0.150	0.096	12	12	11	3.46
11344	T 29	166.991301	−77.645848	10.147	8.406	7.107	0.262	0.182	0.136	11	11	11	5.49
11351	T 30	166.991957	−77.711505	12.017	10.723	9.917	0.200	0.146	0.103	11	11	11	4.21
11462	T 31	167.006145	−77.708036	8.692	7.640	6.947	0.083	0.083	0.090	18	15	17	2.60
11529	ISO 126	167.012202	−77.645213	11.574	9.636	8.205	0.095	0.093	0.070	16	18	20	2.36
11547	T 32	167.013579	−77.654898	7.351	6.926	6.273	0.053	0.068	0.100	21	20	21	1.69
12029	...	167.061355	−79.484326	13.545	13.191	13.125	0.064	0.061	0.079	24	24	24	1.43
12055	T 33	167.063875	−77.564862	8.356	7.189	6.182	0.119	0.114	0.089	19	25	25	2.85
12608	...	167.118568	−74.652561	14.263	13.777	13.643	0.064	0.078	0.103	25	25	25	1.20
12865	...	167.140347	−74.042462	13.034	12.547	12.426	0.083	0.086	0.089	25	25	25	2.70
13058	T 35	167.162555	−77.267845	11.265	9.931	9.045	0.320	0.200	0.120	25	25	24	6.31
13577	...	167.213993	−77.277374	13.478	12.760	12.479	0.102	0.090	0.099	25	25	25	2.60
13616	T 36	167.218164	−76.733232	13.535	12.993	12.809	0.165	0.123	0.113	24	25	24	3.19
13620	RX J1108.8-7519b	167.218439	−75.317429	10.521	9.711	9.365	0.085	0.051	0.045	15	16	15	1.46
13677	PU Car	167.223694	−75.360005	10.943	10.015	9.487	0.097	0.089	0.082	14	15	15	2.46
13707	T 38	167.227553	−77.036964	11.448	10.304	9.549	0.162	0.114	0.067	24	25	24	2.82
13720	ISO 165	167.229063	−76.544769	13.137	12.164	11.523	0.100	0.083	0.051	23	24	21	2.17

Table 3—Continued

ID	Name	Coordinates (J2000)		Mean Magnitudes			Observed RMS			N			Variability
		α	δ	J	H	K_s	J	H	K_s	J	H	K_s	Index
14235	ISO 177	167.282989	−76.819620	12.771	11.945	11.658	0.187	0.154	0.156	13	13	13	5.38
14623	CHXR 79	167.325619	−76.508128	11.785	10.204	9.199	0.082	0.060	0.083	13	13	13	1.86
14800	C 1-6	167.344441	−76.575584	12.737	10.392	8.769	0.259	0.185	0.149	13	13	13	4.53
14843	T 40	167.349170	−76.389109	10.064	8.986	8.121	0.164	0.144	0.124	13	12	13	4.43
15044	ISO 192	167.368966	−76.557816	16.108	13.320	11.044	0.140	0.126	0.105	13	13	13	1.54
15415	...	167.407585	−74.494542	13.069	12.657	12.533	0.055	0.074	0.061	13	13	13	1.59
15576	C 1-25	167.424641	−76.582928	13.764	11.405	10.075	0.082	0.058	0.067	21	19	21	1.52
15771	...	167.445696	−78.339541	12.647	12.237	12.103	0.098	0.098	0.102	24	24	24	2.53
15784	B 43	167.447392	−77.441459	12.592	11.085	10.136	0.205	0.159	0.125	25	24	24	4.23
15991	...	167.468918	−77.676413	15.672	14.386	13.532	0.195	0.173	0.186	25	25	25	1.77
16026	T 42	167.472503	−76.573776	9.612	8.032	6.782	0.246	0.164	0.144	25	25	25	4.82
16052	T 43	167.475246	−76.490380	11.280	10.019	9.311	0.093	0.068	0.049	25	25	25	1.56
16067	ISO 225	167.476587	−76.519830	15.064	13.763	12.971	0.109	0.086	0.130	25	25	25	1.38
16096	C 1-2	167.479373	−76.544746	14.121	11.563	9.787	0.225	0.172	0.116	22	25	25	3.49
16254	T 45	167.494498	−77.619185	9.948	8.863	8.099	0.078	0.065	0.087	25	25	25	2.00
16307	T 44	167.500391	−76.582762	8.777	7.319	6.180	0.073	0.063	0.043	25	25	25	1.35
16442	...	167.515876	−75.894432	12.529	12.320	12.231	0.109	0.116	0.118	25	25	25	3.01
16470	T 45a	167.519496	−76.595892	10.530	9.609	9.221	0.069	0.069	0.060	25	25	25	1.86
17205	...	167.595185	−74.218745	14.615	13.946	13.774	0.251	0.214	0.257	12	17	12	4.03
18261	T 47	167.706551	−77.297735	11.398	10.094	9.311	0.095	0.071	0.070	12	12	12	1.68
18403	T 48	167.722205	−76.575567	11.214	10.445	9.956	0.046	0.037	0.051	12	12	12	1.11
18416	ISO 256	167.723233	−77.416833	13.999	12.242	11.156	0.398	0.312	0.219	12	11	12	8.11
18903	...	167.770410	−74.765601	15.042	14.389	14.206	0.110	0.141	0.115	12	12	12	0.94
18981	...	167.777547	−79.293338	14.230	13.502	13.289	0.092	0.089	0.100	25	25	25	1.68
19580	...	167.836748	−79.286170	13.546	13.355	13.262	0.077	0.061	0.070	25	25	25	1.41
20217	CHXR 48	167.894737	−76.605928	10.757	9.982	9.720	0.072	0.081	0.071	25	24	25	2.27
20409	T 49	167.915282	−76.337519	10.552	9.718	9.180	0.072	0.102	0.135	25	25	25	2.25
21473	ISO 282	168.014564	−77.433591	13.286	12.323	11.682	0.314	0.226	0.152	25	25	22	6.73
21658	...	168.032510	−75.704201	12.990	12.732	12.674	0.135	0.134	0.138	13	13	13	3.64
21687	XZ Cha	168.035605	−78.911010	6.405	5.496	5.010	0.063	0.065	0.039	22	22	22	1.80
21745	T 50	168.041012	−76.576841	11.108	10.296	9.870	0.113	0.117	0.073	13	13	13	3.37
22193	...	168.086269	−77.207763	14.549	13.838	13.567	0.129	0.086	0.131	13	13	13	1.92
22321	...	168.098276	−74.292164	13.685	13.249	13.141	0.145	0.154	0.144	13	13	13	3.38
22521	T 52	168.115452	−76.739550	8.326	7.497	6.865	0.044	0.060	0.067	13	13	13	1.76
22662	T 53	168.128869	−76.740037	10.975	9.878	9.209	0.234	0.154	0.106	13	13	13	4.16
22699	...	168.132021	−75.106479	14.523	14.222	14.152	0.171	0.130	0.136	13	13	13	1.95
23372	...	168.196514	−74.035743	14.317	13.907	13.834	0.098	0.112	0.119	13	13	13	1.56
25420	T 55	168.389819	−76.593759	11.638	11.012	10.727	0.044	0.054	0.048	25	25	25	0.83
26688	...	168.505599	−78.862428	13.249	12.819	12.684	0.143	0.096	0.107	12	12	12	2.77
26728	YY Cha	168.509821	−76.909537	6.338	5.395	4.891	0.110	0.101	0.060	12	10	10	2.72
26963	...	168.532497	−76.602589	14.163	13.611	13.457	0.103	0.085	0.095	12	12	12	0.53
28089	...	168.636947	−76.712773	15.432	14.840	14.690	0.143	0.144	0.160	25	25	25	0.83
29102	...	168.730184	−77.759616	12.813	12.134	11.945	0.054	0.060	0.058	25	24	25	1.17
29730	...	168.783302	−79.022424	9.975	9.078	8.640	0.078	0.068	0.071	24	24	24	1.58
32775	...	169.066868	−74.273598	14.983	14.348	14.208	0.209	0.189	0.216	14	14	14	2.78
32930	...	169.080062	−74.427344	14.921	14.477	14.376	0.198	0.205	0.194	14	14	14	2.26
33139	...	169.097543	−74.461542	13.910	13.553	13.495	0.089	0.095	0.091	14	14	14	1.66

Table 4. New Candidate Members of Chamaeleon I

ID	Coordinates (J2000)		Mean Magnitudes			Observed RMS			Variable?	JHK_s	Name
	α	δ	J	H	K_s	J	H	K_s		excess?	
1715	166.017772	-76.659153	12.906	11.651	10.837	0.203	0.161	0.129	Y	Y	
1982	166.044294	-76.213627	13.141	12.522	12.125	0.016	0.044	0.015		Y	
7869	166.636396	-76.422525	14.270	13.597	13.153	0.049	0.065	0.043		Y	
9484	166.799142	-76.430582	13.667	12.904	12.466	0.066	0.054	0.041	Y		
10193	166.874272	-77.417151	12.163	11.353	10.958	0.121	0.112	0.111	Y		
10862	166.944190	-76.254861	13.972	13.031	12.374	0.045	0.047	0.040		Y	GK 18
11564	167.014837	-79.376292	14.459	13.483	12.265	0.052	0.043	0.041		Y	
13788	167.236477	-77.724595	15.256	13.513	12.449	0.214	0.116	0.052		Y	Cam2 35
15991	167.468918	-77.676413	15.672	14.386	13.532	0.195	0.173	0.186	Y	Y	
17173	167.592793	-76.420500	13.618	12.947	12.485	0.041	0.049	0.030		Y	

Table 5. Near-infrared Photometry for Previously Identified Chamaeleon I Members

Name	Coordinates (J2000)		Mean Magnitudes[a]			RMS[a]			N			Variability	YSO[b]
	α	δ	J	H	K_s	J	H	K_s	J	H	K_s	Index	Properties
T 1	10:52:01.30	-77:09:50.1	13.942	13.333	13.112	0.027	0.037	0.037	1	1	1	...	0Y0000
IRAS 10529-7638	10:54:11.6	-76:54:33	...	...	...	...	...	...	...	...	...	...	00000Y
T 2	10:54:13.32	-77:55:09.2	12.251	11.699	11.477	0.023	0.026	0.029	1	1	1	...	Y00000
T 3	10:55:59.9	-77:24:38	...	...	...	...	...	...	...	...	...	...	YY000Y
T 4	10:56:30.43	-77:11:39.4	9.966	9.078	8.629	0.021	0.026	0.027	1	1	1	...	YY0Y0Y
T 5	10:57:42.28	-76:59:35.7	10.431	9.496	9.196	0.022	0.026	0.025	1	1	1	...	0Y0000
CHXR 3	10:58:05.61	-77:28:24.0	8.507	7.675	7.392	0.025	0.034	0.023	1	1	1	...	0Y0Y0Y
T 6	10:58:16.84	-77:17:17.1	9.270	8.414	7.783	0.025	0.037	0.026	1	1	1	...	YY0Y0Y
T 7	10:59:01.15	-77:22:40.7	10.146	9.208	8.620	0.023	0.027	0.026	1	1	1	...	YY0Y0Y
T 8	10:59:07.00	-77:01:40.1	8.444	7.760	7.351	0.019	0.040	0.014	1	1	1	...	0Y0Y0Y
T 9	11:00:14.08	-76:44:15.4	8.855	7.880	7.363	0.011	0.034	0.023	1	1	1	...	0Y000Y
CHXR 8	11:00:14.54	-77:14:38.0	10.062	9.750	9.655	0.028	0.027	0.026	1	1	1	...	00?Y0Y
T 10	11:00:40.27	-76:19:28.0	11.848	11.242	10.851	0.026	0.026	0.026	1	1	1	...	0Y0000
CHXR 9C	11:01:18.77	-76:27:02.5	10.032	9.303	9.024	0.027	0.027	0.026	1	1	1	...	0YYY00
B 23	11:01:46.6	-77:43:51	...	...	...	...	...	...	...	...	...	...	00000Y
B 9	11:02:15.4	-77:10:59	...	...	...	...	...	...	...	...	...	...	00000Y
ISO 1	11:02:16.3	-77:46:30	...	...	...	...	...	...	...	...	...	...	0000Y0
T 11	11:02:24.92	-77:33:35.8	9.094	8.417	8.232	0.020	0.026	0.016	1	1	1	...	YY0YYY
CHXR 71	11:02:32.67	-77:29:13.0	11.230	10.422	10.076	0.027	0.026	0.024	1	1	1	...	0Y?YYY
ISO 13	11:02:53.1	-77:24:07	...	...	...	...	...	...	...	...	...	...	0000Y0
T 12	11:02:55.06	-77:21:50.9	11.559	10.847	10.449	0.027	0.026	0.026	1	1	1	...	0Y0000
CHXR 11	11:03:11.61	-77:21:04.3	8.156	7.474	7.253	0.021	0.036	0.008	1	1	1	...	00?Y0Y
ISO 28	11:03:41.85	-77:26:52.1	12.921	12.111	11.646	0.026	0.033	0.026	11	9	11	0.04	0000Y0
Hn 2	11:03:47.66	-77:19:56.4	11.353	10.449	10.044	0.044	0.051	0.048	11	9	11	1.27	YY000Y
T 13	11:03:51.01	-76:55:45.6	14.374	14.049	13.942	0.067	0.052	0.062	11	9	11	0.30	Y00000
CHXR 12	11:03:56.83	-77:21:33.0	10.776	10.001	9.709	0.022	0.033	0.023	11	9	11	0.33	0YYY0Y
T 14	11:04:09.11	-76:27:19.3	9.668	8.935	8.563	0.056	0.063	0.067	11	9	11	1.47	YY0Y0Y
CHXR 72	11:04:11.06	-76:54:32.2	11.845	11.174	10.959	0.031	0.025	0.024	11	9	11	0.25	0Y0Y00
T 14a	11:04:22.78	-77:18:08.2	14.335	13.154	12.253	0.066	0.069	0.038	11	9	11	0.53	0000YY
T 15	11:04:24.26	-77:25:48.8	10.980	10.069	9.589	0.025	0.028	0.028	11	9	11	0.19	0Y0000
ISO 52	11:04:42.59	-77:41:57.1	11.793	11.022	10.621	0.023	0.019	0.037	11	9	11	0.06	0000YY
CHXR 14N	11:04:51.03	-76:25:24.0	10.535	9.822	9.604	0.025	0.029	0.019	11	9	11	0.36	0YYY00
CHXR 14S	11:04:52.87	-76:25:51.5	10.695	9.931	9.716	0.031	0.033	0.028	11	9	11	0.83	0YYY00
T 16	11:04:57.00	-77:15:57.0	12.245	10.974	10.498	0.448	0.296	0.359	11	9	11	7.83	YY00YY
B 29	11:05:01.9	-77:41:31	...	...	...	...	...	...	...	...	...	...	00000Y
Hn 4	11:05:14.64	-77:11:29.2	10.913	9.976	9.590	0.025	0.026	0.023	11	9	11	0.30	0Y0000
T 18	11:05:15.23	-77:52:54.7	13.054	11.912	11.475	0.031	0.024	0.031	11	9	11	0.28	0Y0000
T 17	11:05:21.60	-76:30:21.6	13.254	12.781	12.653	0.032	0.033	0.037	11	9	11	0.08	Y00000
T 19	11:05:41.57	-77:54:44.0	11.346	10.752	10.598	0.020	0.030	0.020	11	9	11	0.10	0Y0000
CHXR 15	11:05:42.97	-77:26:51.7	11.216	10.555	10.208	0.023	0.032	0.032	11	9	11	0.44	0Y0Y0Y
T 20	11:05:52.62	-76:18:25.5	10.249	9.543	9.311	0.032	0.038	0.031	11	9	11	0.78	YY0Y00
ISO 68	11:05:53.93	-77:43:27.2	13.464	12.372	11.896	0.038	0.032	0.034	11	9	11	0.47	0000Y0
ISO 71	11:06:04.06	-77:39:23.8	15.309	13.621	12.915	0.065	0.039	0.026	11	9	11	0.10	0000Y0
T 21	11:06:15.36	-77:21:56.7	7.614	6.811	6.445	0.016	0.021	0.012	11	9	11	0.26	0YYYYY
B 31	11:06:26.4	-77:34:20	...	...	...	...	...	...	...	...	...	...	00000Y
CHXR 73	11:06:28.72	-77:37:33.2	12.628	11.269	10.689	0.045	0.025	0.031	11	9	11	0.41	000Y0Y
Cha Ha 12	11:06:37.93	-77:43:09.2	12.997	12.281	11.818	0.038	0.032	0.027	11	9	11	0.31	0Y00Y0
ISO 79	11:06:39.42	-77:36:05.3	14.962	13.367	12.321	0.064	0.050	0.039	11	9	11	0.57	0000Y0

Table 5—Continued

Name	Coordinates (J2000)		Mean Magnitudes[a]			RMS[a]			N			Variability	YSO[b]
	α	δ	J	H	K_s	J	H	K_s	J	H	K_s	Index	Properties
Hn 5	11:06:41.76	-76:35:49.2	11.588	10.727	10.177	0.072	0.059	0.039	11	9	11	1.19	YY00Y0
T 22	11:06:43.43	-77:26:34.5	10.753	9.718	9.347	0.033	0.033	0.031	11	9	11	0.46	Y00000
CHXR 20	11:06:45.05	-77:27:02.5	10.717	9.628	9.134	0.617	0.458	0.334	11	9	11	12.42	YYYYYY
Ced 110 IRS4	11:06:46.23	-77:22:29.0	...	15.337	13.087	...	0.126	0.244	11	9	11	−0.52	00000Y
CHXR 74	11:06:57.29	-77:42:10.6	11.431	10.589	10.217	0.032	0.038	0.023	11	9	11	0.15	0Y?Y0Y
ISO 86	11:06:58.01	-77:22:48.8	...	...	13.458	...	...	0.095	11	9	11	0.90	0000Y0
T 23	11:06:59.01	-77:18:53.5	11.195	10.429	9.999	0.044	0.051	0.049	11	9	11	1.20	YY00YY
Ced 110 IRS6	11:07:09.15	-77:23:05.0	...	14.747	11.010	...	0.097	0.056	11	9	11	0.41	0000YY
ISO 91	11:07:09.19	-77:18:47.1	14.912	12.602	11.445	0.046	0.031	0.035	11	9	11	0.23	0000Y0
CHXR 22W	11:07:10.42	-77:43:44.2	14.042	12.975	12.455	0.030	0.037	0.037	11	9	11	0.06	000YY0
CHXR 21	11:07:11.43	-77:46:39.4	11.077	10.024	9.621	0.016	0.029	0.024	11	9	11	0.09	0Y?Y0Y
T 24	11:07:12.04	-76:32:23.3	10.829	9.837	9.325	0.170	0.145	0.088	11	9	11	3.63	YY0Y00
CHXR 22E	11:07:13.27	-77:43:49.8	11.869	10.558	9.987	0.028	0.036	0.036	11	9	11	0.44	000Y0Y
ISO 97	11:07:16.19	-77:23:06.9	...	13.841	11.451	...	0.134	0.102	11	9	11	1.58	Y000Y0
Cha Ha 1	11:07:16.65	-77:35:53.3	13.356	12.643	12.194	0.027	0.023	0.027	11	9	11	0.16	0Y00Y0
Cha Ha 9	11:07:18.56	-77:32:51.6	13.754	12.481	11.761	0.034	0.037	0.025	11	9	11	0.14	0Y00Y0
T 25	11:07:19.15	-76:03:04.9	10.962	10.090	9.808	0.047	0.049	0.040	11	9	11	0.91	0Y000Y
T 26	11:07:20.72	-77:38:07.3	7.810	6.941	6.224	0.021	0.034	0.040	11	9	11	0.74	YYYYYY
B 35	11:07:21.38	-77:22:11.8	15.283	12.396	10.835	0.059	0.048	0.045	11	9	11	0.38	0000YY
T 27	11:07:28.24	-76:52:11.9	10.686	9.911	9.580	0.030	0.024	0.035	11	9	11	0.39	YY0Y00
CHXR 25	11:07:32.97	-77:28:27.9	11.644	11.032	10.783	0.023	0.023	0.024	11	9	11	0.29	0Y0Y0Y
CHXR 76	11:07:35.16	-77:34:49.5	12.144	11.246	10.892	0.046	0.040	0.038	11	9	11	0.70	0Y0Y0Y
CHXR 26	11:07:36.84	-77:33:33.6	11.618	10.043	9.337	0.054	0.053	0.039	11	9	11	0.65	000Y0Y
Cha Ha 7	11:07:37.72	-77:35:31.0	13.686	12.903	12.395	0.037	0.027	0.026	11	9	11	0.15	0Y00Y0
Cha Ha 2	11:07:42.44	-77:33:59.6	12.218	11.209	10.645	0.023	0.026	0.023	11	9	11	0.06	0Y00Y0
T 28	11:07:43.64	-77:39:41.2	10.196	9.013	8.304	0.043	0.049	0.058	11	9	11	1.20	YY0YYY
Cha Ha 8	11:07:46.07	-77:40:09.0	12.813	12.008	11.530	0.026	0.043	0.021	11	9	11	0.39	0Y0000
ISO 114	11:07:51.15	-77:10:00.1	13.933	13.282	13.084	0.032	0.052	0.038	11	9	11	−0.09	0000Y0
Cha Ha 3	11:07:52.24	-77:36:57.2	12.346	11.571	11.120	0.031	0.037	0.025	11	9	11	0.43	0Y0000
CHXR 28	11:07:55.85	-77:27:25.9	9.119	8.084	7.736	...	0.030	0.028	11	9	11	0.34	0YYY0Y
CHXR 30b	11:07:57.28	-77:17:26.4	13.278	11.119	9.825	0.204	0.150	0.096	11	9	11	3.46	Y00YYY
T 29	11:07:57.91	-77:38:45.1	10.147	8.406	7.107	0.262	0.182	0.136	11	9	11	5.49	YY00YY
T 30	11:07:58.07	-77:42:41.4	12.017	10.723	9.917	0.200	0.146	0.103	11	9	11	4.21	YY00Y0
CHXR 30a	11:07:59.98	-77:17:30.6	11.819	9.958	9.118	0.031	0.017	0.014	11	9	11	0.36	000YYY
T 31	11:08:01.47	-77:42:28.9	8.692	7.640	6.947	0.083	0.083	0.090	11	9	11	2.60	YY0YYY
ISO 126	11:08:02.93	-77:38:42.8	11.574	9.636	8.205	0.095	0.093	0.070	11	9	11	2.36	Y000Y0
T 32	11:08:03.26	-77:39:17.6	7.351	6.926	6.273	0.053	0.068	0.100	11	9	11	1.69	YY0YYY
T 33	11:08:15.33	-77:33:53.5	8.356	7.189	6.182	0.119	0.114	0.089	11	9	11	2.85	YY0YYY
T 34	11:08:16.46	-77:44:37.3	11.186	10.353	10.036	0.036	0.040	0.029	11	9	11	0.54	0Y000Y
Cha Ha 13	11:08:17.01	-77:44:12.0	11.792	11.045	10.660	0.037	0.035	0.022	11	9	11	0.37	0Y0000
B 40	11:08:17.9	-77:32:22	...	...	...	...	...	...	...	...	...	...	00000Y
ISO 138	11:08:18.44	-77:30:41.0	14.054	13.464	13.051	0.046	0.039	0.048	11	9	11	−0.02	0Y00Y0
Cha Ha 4	11:08:18.93	-77:39:17.3	12.115	11.443	11.041	0.037	0.036	0.027	11	9	11	0.49	0Y0000
ISO 143	11:08:22.33	-77:30:27.9	12.601	11.624	11.093	0.053	0.041	0.037	11	9	11	0.69	0Y00Y0
Cha Ha 10	11:08:24.02	-77:39:30.2	14.322	13.670	13.222	0.044	0.051	0.040	11	9	11	0.22	0Y00Y0
Cha Ha 5	11:08:24.08	-77:41:47.6	12.040	11.185	10.736	0.028	0.030	0.032	11	9	11	0.28	0Y0000
ISO 145	11:08:25.77	-76:55:57.0	13.737	12.911	12.582	0.040	0.043	0.039	11	9	11	0.25	0000Y0
ISO 147	11:08:26.45	-77:15:55.2	13.712	12.903	12.372	0.043	0.039	0.042	11	9	11	0.65	0000Y0

Table 5—Continued

Name	Coordinates (J2000)		Mean Magnitudes[a]			RMS[a]			N			Variability	YSO[b]
	α	δ	J	H	K_s	J	H	K_s	J	H	K_s	Index	Properties
Cha Ha 11	11:08:29.23	-77:39:19.9	14.598	13.947	13.507	0.067	0.050	0.054	11	9	11	0.27	0Y0000
IRN	11:08:38.95	-77:43:51.4	11.934	9.896	8.521	0.173	0.108	0.055	11	9	11	...	0000YY
T 35	11:08:39.01	-77:16:04.2	11.265	9.931	9.045	0.320	0.200	0.120	11	9	11	6.31	YY00YY
Cha Ha 6	11:08:39.49	-77:34:16.8	12.270	11.497	11.026	0.032	0.030	0.026	11	9	11	0.28	0Y00Y0
CHXR 33	11:08:40.70	-76:36:07.9	10.587	9.650	9.295	0.029	0.032	0.023	11	9	11	0.34	0YYY00
ISO 154	11:08:43.05	-76:27:46.8	12.749	11.764	11.453	0.029	0.026	0.032	11	9	11	0.21	0000Y0
T 37	11:08:50.92	-76:25:13.7	12.404	11.729	11.332	0.027	0.037	0.028	11	9	11	0.19	0Y00Y0
T 36	11:08:52.36	-76:43:59.6	13.535	12.993	12.809	0.165	0.123	0.113	11	9	11	3.19	Y00000
CHXR 78C	11:08:54.19	-77:32:11.7	12.350	11.566	11.187	0.021	0.031	0.032	11	9	11	0.30	0Y0YYY
T 38	11:08:54.61	-77:02:13.1	11.448	10.304	9.549	0.162	0.114	0.067	11	9	11	2.82	YY00Y0
ISO 164	11:08:54.75	-76:39:41.6	12.397	11.848	11.686	0.028	0.032	0.028	11	9	11	0.39	0000Y0
ISO 165	11:08:54.98	-76:32:41.2	13.137	12.164	11.523	0.100	0.083	0.051	11	9	11	2.17	Y000Y0
Hn 7	11:09:05.10	-77:09:58.0	11.937	11.261	10.987	0.016	0.030	0.020	11	9	11	0.13	0Y0000
ISO 177	11:09:07.92	-76:49:10.6	12.771	11.945	11.658	0.187	0.154	0.156	11	9	11	5.38	Y000Y0
T 39	11:09:11.71	-77:29:12.6	9.877	9.058	8.887	0.045	0.090	0.047	11	9	11	...	0Y0Y0Y
CHXR 35	11:09:13.84	-76:28:39.6	11.849	11.185	10.894	0.027	0.035	0.022	11	9	11	0.16	0Y0Y00
OTS 7	11:09:16.5	-76:36:39	...	...	...	...	...	...	...	...	...	...	0000Y0
CHXR 37	11:09:17.72	-76:27:57.8	10.017	9.041	8.700	0.018	0.029	0.021	11	9	11	−0.01	0YYY00
CHXR 79	11:09:18.15	-76:30:29.3	11.785	10.204	9.199	0.082	0.060	0.083	11	9	11	1.86	YY0YY0
C 1-6	11:09:22.67	-76:34:32.1	12.737	10.392	8.769	0.259	0.185	0.149	11	9	11	4.53	Y000Y0
T 40	11:09:23.80	-76:23:20.8	10.064	8.986	8.121	0.164	0.144	0.124	11	9	11	4.43	YY0YYY
OTS 11	11:09:24.1	-76:34:55	...	...	...	...	...	...	...	...	...	...	0000Y0
Ced 112 IRS2	11:09:26.05	-76:33:33.8	13.258	11.251	10.237	0.031	0.025	0.026	11	9	11	0.17	00000Y
ISO 192	11:09:28.55	-76:33:28.1	16.108	13.320	11.044	0.140	0.126	0.105	11	9	11	1.54	Y000Y0
CHXR 40	11:09:40.08	-76:28:39.2	10.096	9.209	8.955	0.023	0.028	0.028	11	9	11	0.13	0YYY00
C 1-25	11:09:41.91	-76:34:58.5	13.764	11.405	10.075	0.082	0.058	0.067	11	9	11	1.52	Y000Y0
C 7-1	11:09:42.55	-77:25:58.0	12.319	11.150	10.538	0.042	0.028	0.032	11	9	11	0.43	0000YY
Hn 10W	11:09:43.07	-76:34:38.7	...	15.693	14.663	...	0.161	0.106	11	9	11	−0.14	000000
C 2-3	11:09:45.86	-76:43:54.5	11.820	10.753	10.172	0.052	0.035	0.030	11	9	11	0.45	000000
Hn 10E	11:09:46.19	-76:34:46.5	11.993	10.755	10.114	0.052	0.039	0.035	11	9	11	0.65	0Y00YY
B 43	11:09:47.37	-77:26:29.3	12.592	11.085	10.136	0.205	0.159	0.125	11	9	11	4.23	Y000YY
ISO 206	11:09:47.63	-76:51:18.2	16.503	14.468	13.480	0.139	0.076	0.070	11	9	11	0.17	0000Y0
ISO 209	11:09:48.62	-77:14:38.4	15.404	13.400	12.279	0.069	0.041	0.035	11	9	11	0.22	0000Y0
T 41	11:09:50.01	-76:36:47.7	7.640	7.381	7.188	0.034	0.019	0.022	11	9	11	0.46	000YYY
ISO 216	11:09:51.98	-76:57:58.9	11.873	10.613	10.074	0.033	0.026	0.021	11	9	11	0.32	0000Y0
ISO 217	11:09:52.14	-76:39:12.8	13.538	12.512	11.767	0.050	0.040	0.037	11	9	11	0.51	0000Y0
ISO 220	11:09:53.31	-77:28:36.7	14.316	13.091	12.329	0.046	0.039	0.059	11	9	11	0.80	0Y00Y0
T 42	11:09:53.40	-76:34:25.6	9.612	8.032	6.782	0.246	0.164	0.144	11	9	11	4.82	YY00YY
T 43	11:09:54.06	-76:29:25.4	11.280	10.019	9.311	0.093	0.068	0.049	11	9	11	1.56	YY0YY0
ISO 225	11:09:54.38	-76:31:11.4	15.064	13.763	12.971	0.109	0.086	0.130	11	9	11	1.38	Y000Y0
C 1-2	11:09:55.05	-76:32:41.1	14.121	11.563	9.787	0.225	0.172	0.116	11	9	11	3.49	Y000YY
T 45	11:09:58.68	-77:37:09.1	9.948	8.863	8.099	0.078	0.065	0.087	11	9	11	2.00	YY0YYY
T 44	11:10:00.09	-76:34:57.9	8.777	7.319	6.180	0.073	0.063	0.043	11	9	11	1.35	YY0YY0
OTS 31	11:10:02.4	-76:32:37	...	...	...	...	...	...	...	...	...	...	0000Y0
OTS 32	11:10:03.35	-76:33:11.1	16.674	15.020	13.873	0.189	0.108	0.069	11	9	11	−0.08	0000Y0
Hn 11	11:10:03.69	-76:33:29.2	11.779	10.278	9.478	0.036	0.054	0.053	11	9	11	0.83	0Y00Y0
T 45a	11:10:04.68	-76:35:45.2	10.530	9.609	9.221	0.069	0.069	0.060	11	9	11	1.86	Y00YYY
T 46	11:10:07.04	-76:29:37.6	9.921	8.958	8.475	0.041	0.051	0.048	11	9	11	0.74	YY0YYY

Table 5—Continued

Name	Coordinates (J2000)		Mean Magnitudes[a]			RMS[a]			N			Variability	YSO[b]
	α	δ	J	H	K_s	J	H	K_s	J	H	K_s	Index	Properties
ISO 235	11:10:07.83	-77:27:48.1	13.518	12.075	11.301	0.029	0.032	0.026	11	9	11	0.14	0000Y0
OTS 44	11:10:09.32	-76:32:18.0	16.365	15.317	14.602	0.157	0.163	0.093	11	9	11	−0.05	0000Y0
OTS 42	11:10:09.34	-76:35:06.4	15.413	14.035	13.393	0.063	0.045	0.064	11	9	11	0.04	0000Y0
ISO 237	11:10:11.40	-76:35:29.2	10.908	9.448	8.678	0.040	0.032	0.040	11	9	11	0.79	0000Y0
OTS 48	11:10:14.1	-76:34:37	...	...	...	...	...	...	...	...	...	...	0000Y0
Hn 12W	11:10:28.50	-77:16:59.6	11.716	11.059	10.728	0.028	0.031	0.030	11	9	11	0.13	0Y0000
OTS 56	11:10:30.0	-76:32:53	...	...	...	...	...	...	...	...	...	...	0000Y0
Hn 12E	11:10:30.67	-77:17:00.9	15.914	14.835	14.404	0.126	0.076	0.094	11	9	11	0.07	000000
OTS 59	11:10:32.0	-76:35:55	...	...	...	...	...	...	...	...	...	...	0000Y0
ISO 247	11:10:33.68	-76:39:22.4	13.245	11.947	11.347	0.028	0.034	0.032	11	9	11	0.27	0000Y0
ISO 250	11:10:36.42	-77:22:13.1	12.730	11.339	10.674	0.020	0.030	0.022	11	9	11	0.09	0000Y0
CHXR 47	11:10:38.00	-77:32:40.0	9.711	8.686	8.259	0.030	0.033	0.038	11	9	11	0.46	0YYYYY
ISO 252	11:10:41.40	-77:20:48.1	13.885	12.886	12.285	0.026	0.038	0.026	11	9	11	0.00	0Y00Y0
OTS 61	11:10:42.9	-76:34:05	...	...	...	...	...	...	...	...	...	...	0000Y0
T 47	11:10:49.57	-77:17:51.8	11.398	10.094	9.311	0.095	0.071	0.070	11	9	11	1.68	YY00YY
T 48	11:10:53.33	-76:34:32.0	11.214	10.445	9.956	0.046	0.037	0.051	11	9	11	1.11	YY0YY0
ISO 256	11:10:53.58	-77:25:00.6	13.999	12.242	11.156	0.398	0.312	0.219	11	9	11	8.11	YY00Y0
Hn 13	11:10:55.96	-76:45:32.6	11.244	10.419	9.919	0.049	0.048	0.029	11	9	11	0.85	0Y00Y0
B 47	11:11:09.1	-77:26:19	...	...	...	...	...	...	...	...	...	...	00000Y
Hn 14	11:11:14.17	-76:41:11.1	14.128	12.996	12.612	0.049	0.045	0.038	11	9	11	0.27	0Y0000
ISO 274	11:11:25.48	-77:06:10.2	14.389	13.621	13.274	0.051	0.048	0.053	11	9	11	0.24	0000Y0
CHXR 48	11:11:34.74	-76:36:21.3	10.757	9.982	9.720	0.072	0.081	0.071	11	9	11	2.27	YYYY00
T 49	11:11:39.67	-76:20:15.1	10.552	9.718	9.180	0.072	0.102	0.135	11	9	11	2.25	YY00YY
CHX 18N	11:11:46.34	-76:20:09.0	9.082	8.304	7.833	0.037	0.038	0.041	11	9	11	0.85	0YYY0Y
CHXR 49NE	11:11:54.01	-76:19:30.9	10.197	9.446	9.179	0.018	0.034	0.028	11	9	11	0.29	0YYY00
CHXR 84	11:12:03.28	-76:37:03.3	11.736	11.092	10.748	0.028	0.034	0.029	11	9	11	0.49	0Y0Y00
ISO 282	11:12:03.50	-77:26:00.9	13.286	12.323	11.682	0.314	0.226	0.152	11	9	11	6.73	Y000Y0
T 50	11:12:09.84	-76:34:36.6	11.108	10.296	9.870	0.113	0.117	0.073	11	9	11	3.37	YY0Y00
T 51	11:12:24.41	-76:37:06.5	9.201	8.431	8.021	0.041	0.021	0.026	11	9	11	−0.10	0Y0Y0Y
T 52	11:12:27.71	-76:44:22.4	8.326	7.497	6.865	0.044	0.060	0.067	11	9	11	1.76	YY0YYY
CHXR 53	11:12:27.75	-76:25:29.3	10.887	10.208	9.980	0.022	0.025	0.030	11	9	11	0.28	0Y0Y00
T 53	11:12:30.93	-76:44:24.1	10.975	9.878	9.209	0.234	0.154	0.106	11	9	11	4.16	YY00Y0
CHXR 54	11:12:42.10	-76:58:40.1	10.422	9.699	9.500	0.034	0.045	0.036	11	9	11	0.74	0YYY00
T 54	11:12:42.67	-77:22:23.0	8.625	8.033	7.861	0.020	0.027	0.018	11	9	11	0.16	0Y0Y0Y
CHXR 55	11:12:42.98	-76:37:05.0	10.039	9.397	9.251	0.025	0.034	0.039	11	9	11	0.70	0YYY00
Hn 17	11:12:48.59	-76:47:06.7	12.087	11.425	11.151	0.039	0.037	0.045	11	9	11	0.89	0Y0000
CHXR 57	11:13:20.13	-77:01:04.4	10.938	10.220	9.985	0.035	0.034	0.026	11	9	11	0.53	0YYY0Y
Hn 18	11:13:24.45	-76:29:22.9	11.848	11.106	10.764	0.024	0.033	0.047	11	9	11	0.22	0Y0000
CHXR 59	11:13:27.36	-76:34:16.7	10.584	9.853	9.621	0.030	0.035	0.033	11	9	11	0.53	0YYY00
CHXR 60	11:13:29.69	-76:29:01.4	11.554	10.839	10.552	0.023	0.028	0.027	11	9	11	0.10	0Y0Y00
IRAS 11120-7750	11:13:30.32	-78:07:02.4	6.804	5.783	5.346	0.035	0.028	0.028	11	9	11	0.98	00000Y
T 55	11:13:33.56	-76:35:37.5	11.638	11.012	10.727	0.044	0.054	0.048	11	9	11	0.83	YY0Y00
CHXR 62	11:14:15.64	-76:27:36.6	11.257	10.443	10.122	0.024	0.024	0.027	11	9	11	0.23	0Y0Y00
Hn 21W	11:14:24.50	-77:33:06.4	11.986	11.049	10.597	0.043	0.036	0.038	11	9	11	0.20	0Y0000
Hn 21E	11:14:26.09	-77:33:04.4	12.754	11.941	11.484	0.036	0.035	0.038	11	9	11	0.20	000000
B 53	11:14:50.30	-77:33:38.8	10.463	9.742	9.496	0.021	0.026	0.027	11	9	11	0.10	00000Y
CHXR 65B	11:16:11.95	-77:14:10.1	14.170	13.619	13.357	0.056	0.027	0.052	11	9	11	0.18	000Y00
CHXR 65A	11:16:12.91	-77:14:06.5	11.061	10.464	10.312	0.039	0.024	0.038	11	9	11	0.28	0Y0Y0Y

Table 5—Continued

Name	Coordinates (J2000)		Mean Magnitudes[a]			RMS[a]			N			Variability	YSO[b]
	α	δ	J	H	K_s	J	H	K_s	J	H	K_s	Index	Properties
T 56	11:17:36.95	-77:04:38.0	10.293	9.562	9.267	0.024	0.027	0.028	1	1	1	...	0Y0Y0Y
CHXR 68B	11:18:19.54	-76:22:01.4	11.264	10.539	10.297	0.028	0.026	0.029	1	1	1	...	000Y00
CHXR 68A	11:18:20.21	-76:21:57.7	9.772	9.063	8.829	0.026	0.027	0.030	1	1	1	...	0YYY00
IRAS 11248-7653	11:26:41.5	-77:10:15	...	...	...	...	...	...	...	...	...	...	00000Y

[a]For sources with J, H, and K_s photometry, N=1 in all three bands, but otherwise no tabulated Stetson index, the photometry is from the Version 2 processing of the 2MASS Working Database and the RMS represents the photometric uncertainty from the 2MASS processing pipeline.

[b]Six character flag indicating the properties of that star. References provided in the text.

First character : Variable identified from this study or General Catalog of Variable Stars

Second character: Contains Hα in emission

Third character : Contains lithium in absorption

Fourth character: X-ray source

Fifth character : Contains an infrared excess

Sixth character : Far-infrared source

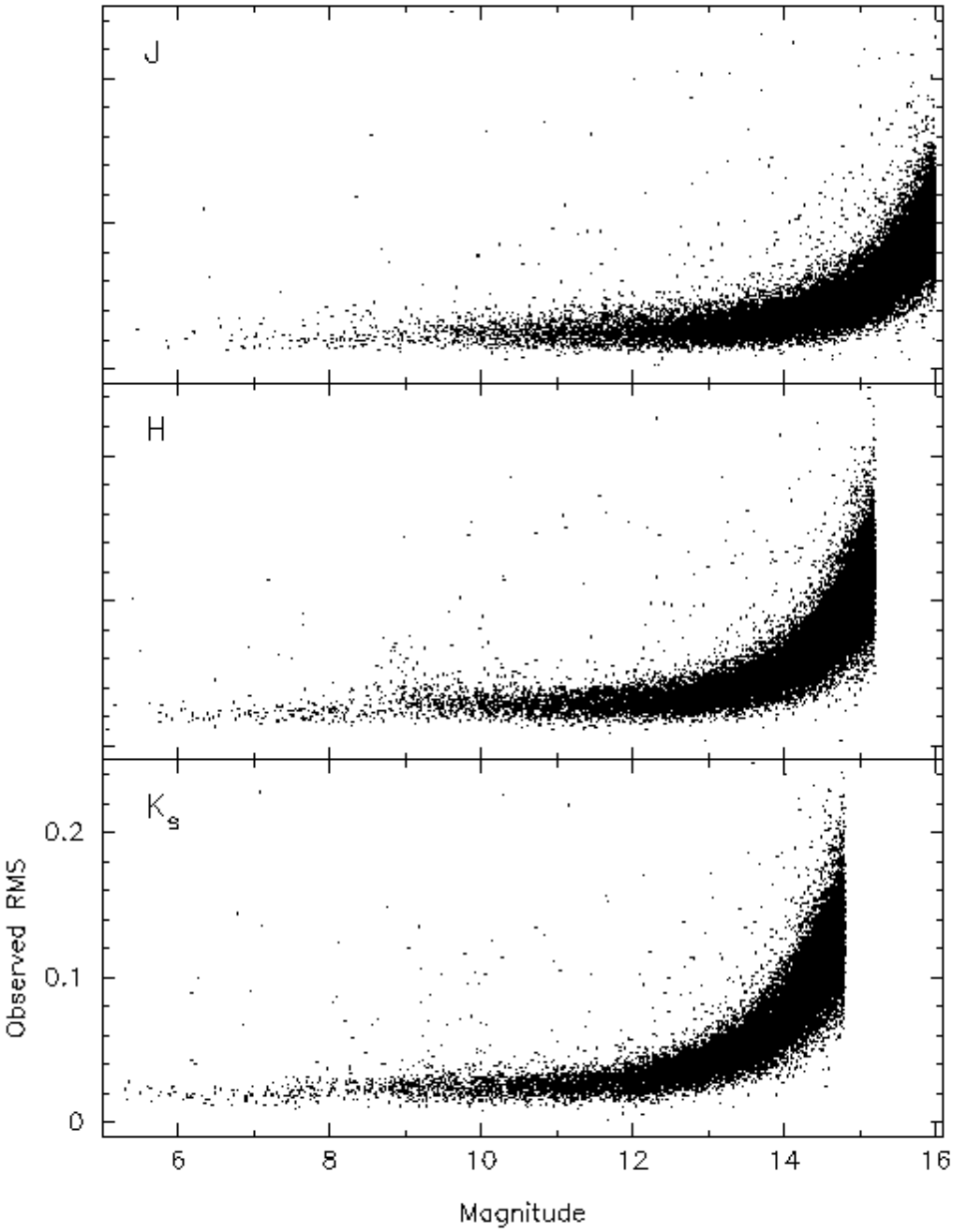

Fig. 1.— The observed photometric RMS in the time series data as a function of magnitude for stars brighter than the defined completeness limits. The observed RMS ranges from ~ 0.020 mag for the brightest stars to $\lesssim 0.15$ mag (i.e. signal to noise ratio ≥ 7) for stars at the completeness limit. The scale on the y-axis is the same for each panel.

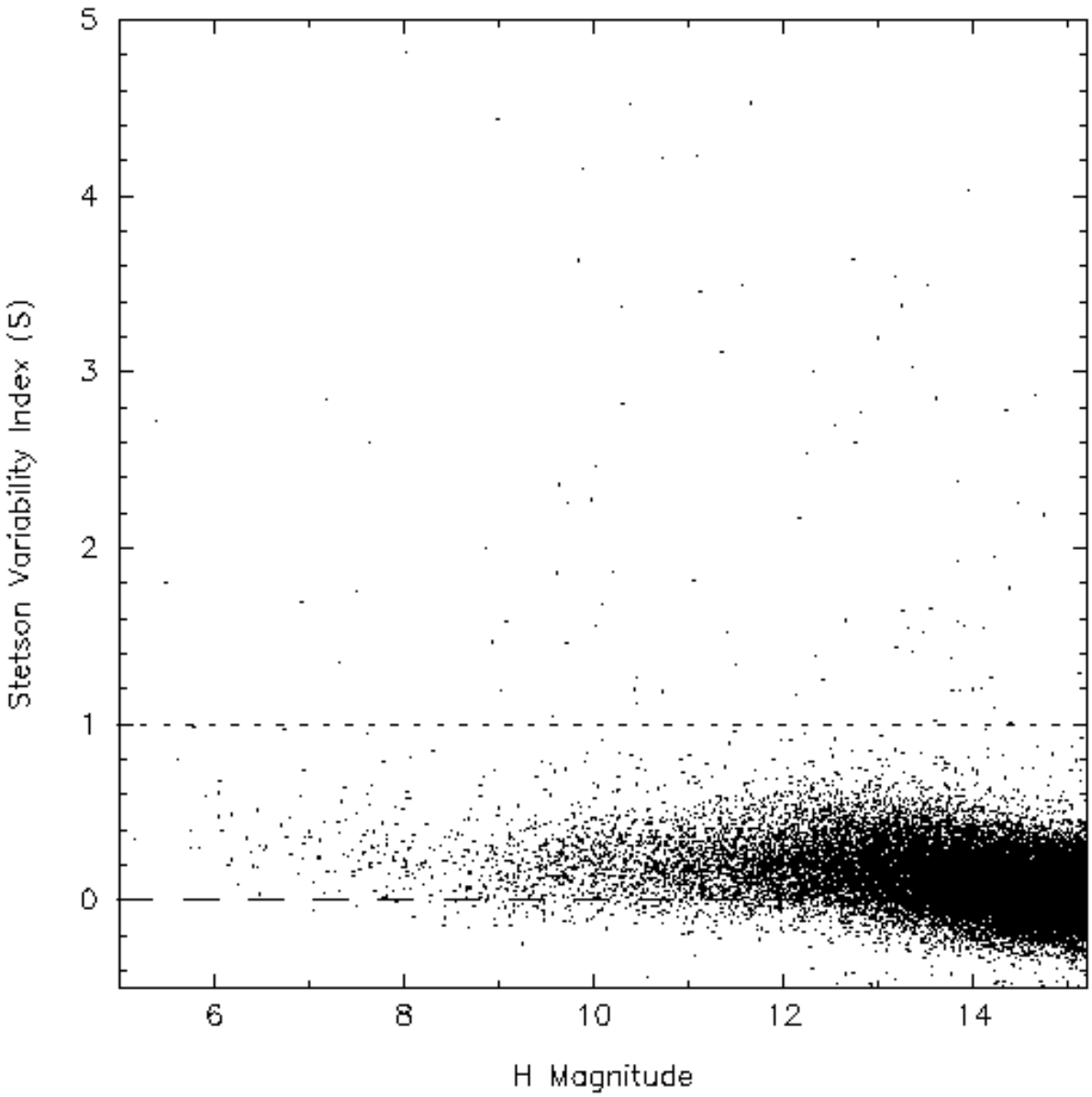

Fig. 2.— The Stetson variable index (S) plotted as a function of the H magnitude for stars brighter than H=15.2. The dashed line at $S = 0$ shows the expected value of the variability index for non-variable stars. The origin of the positive bias in the computed index values is unknown, and suggests that a weak correlation exists between the J, H, and K_s photometry, possibly from the fact that the three bands were observed at the same time. The dotted line at $S = 1.00$ represents the minimum adopted value used to identify variable stars in this study. Note that 7 stars with $S > 5.0$ are not shown.

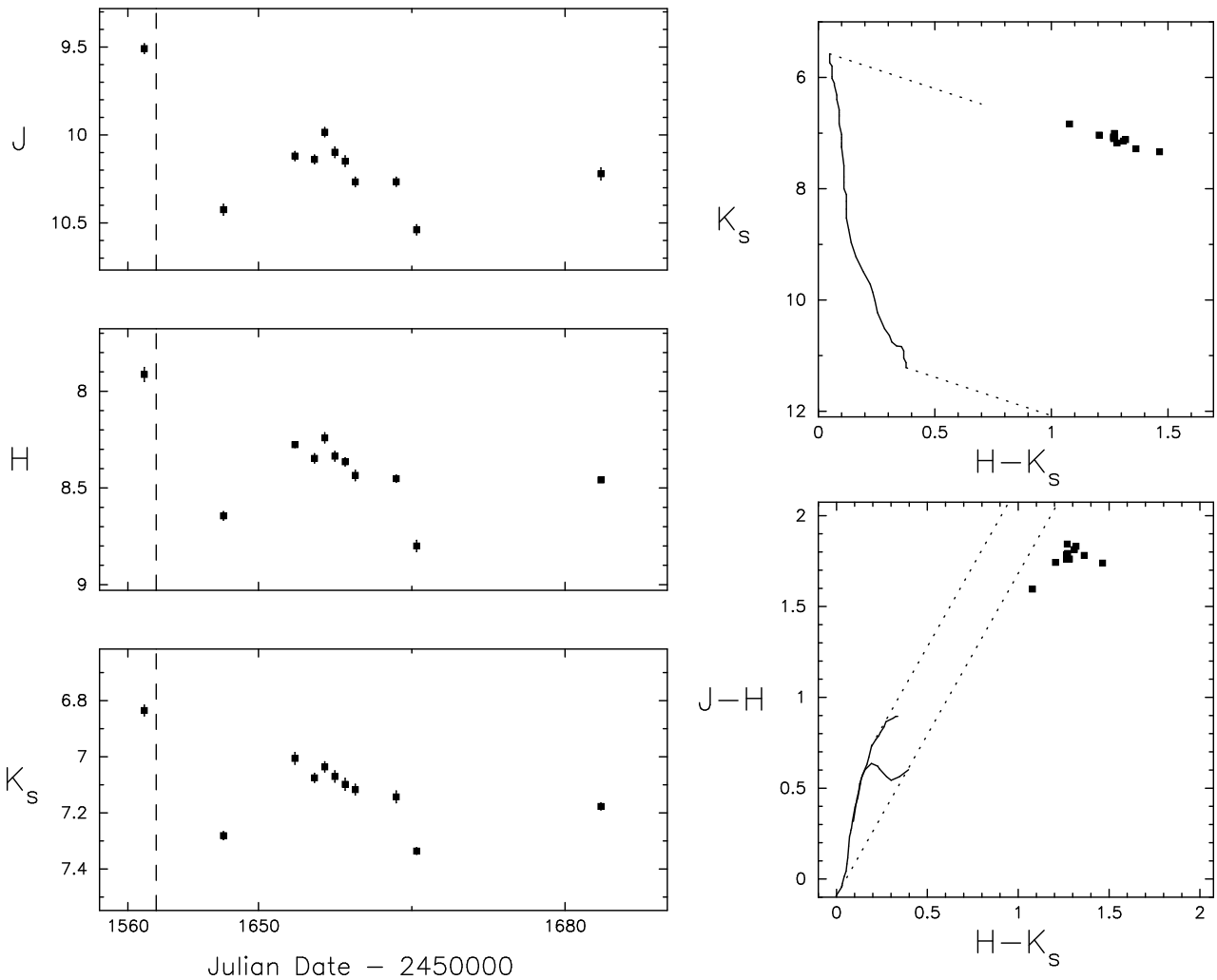

Fig. 3.— Photometric data for star 11344 (also known as T 29 and Sz 22) that illustrates the data obtained for this study. The left and middle panels show the J, H, K_s, $J-H$ and $H-K_s$ light curves. The vertical bars through the data points represent the $\pm 1\sigma$ photometric uncertainties. The right panels show the K_s vs. $H-K_s$ color-magnitude diagram and the $J-H$ vs. $H-K_s$ color-color diagrams for each data point in the time series, where the dotted line represents the interstellar reddening vector from Cohen et al. (1981) transformed into the 2MASS photometric system (Carpenter 2001). The uncertainties in the stellar colors have been omitted for clarity. The solid line in the color-magnitude diagram is the 2 Myr pre-main-sequence isochrone from D'Antona & Mazzitelli (1997,98) for stellar masses between $0.08\,M_\odot$ and $3\,M_\odot$. The solid curves in the color-color diagram are the loci of red giant and main-sequence stars from Bessell & Brett (1988) in the 2MASS color system.

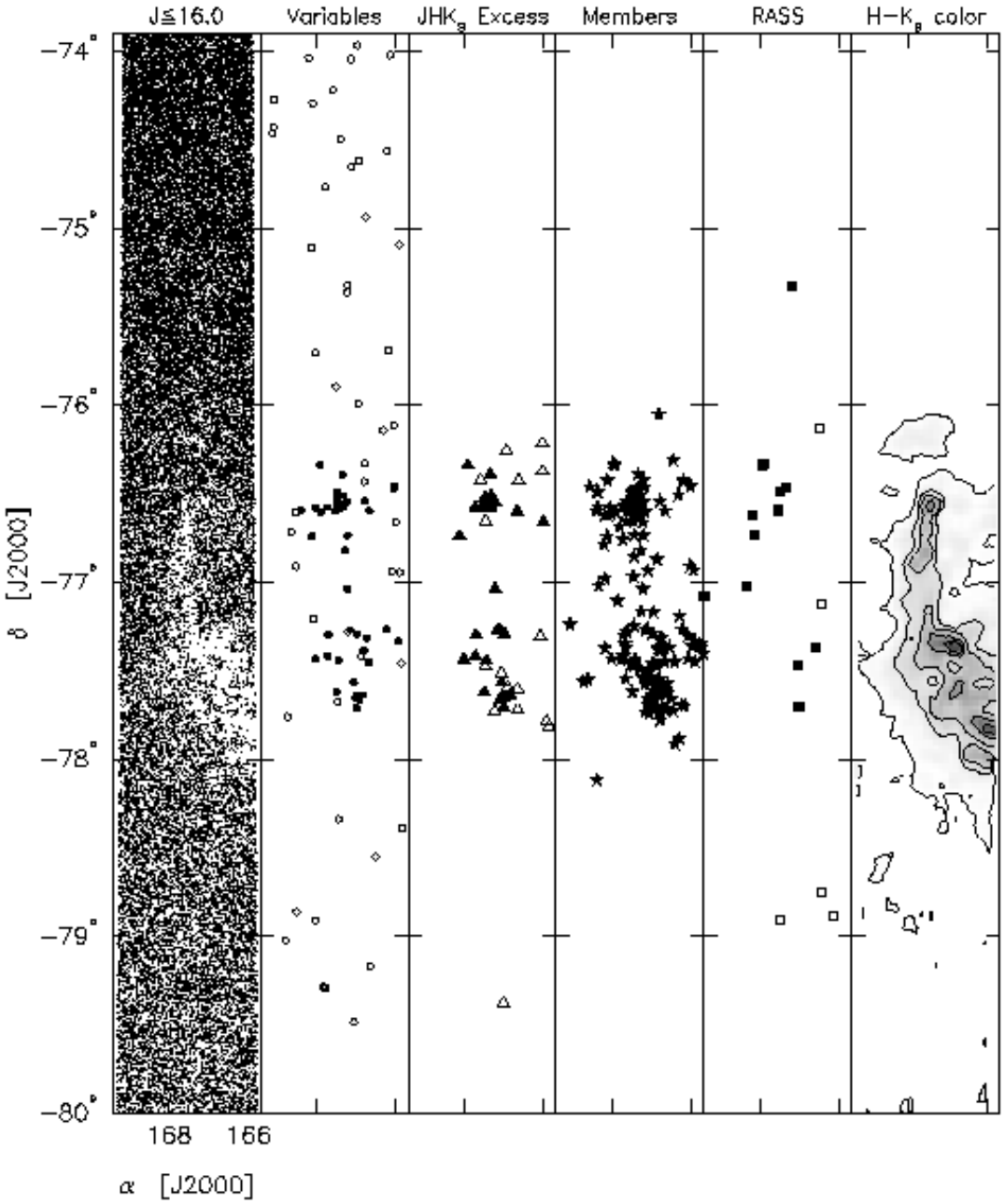

Fig. 4.— Spatial distribution of stars toward the Chamaeleon I molecular cloud. Starting with the leftmost panel, these figures show (*a*) the spatial distribution of sources with $J \leq 16$; (*b*) location of variable stars identified from our near-infrared data, where filled symbols indicate variable stars that were previously identified as Chamaeleon I members; (*c*) sources that exhibit a near-infrared excess in the $J-H$ vs. $H-K_s$ color-color diagram, where filled triangles represent variable stars, and open triangles indicate non-variables brighter than K_s=13.5; (*d*) members and candidate members of the Chamaeleon I molecular cloud identified prior to this study (see Appendix); (*e*) x-ray sources selected from the ROSAT All Sky Survey, where filled squares represent x-ray sources that have been associated with pre-main-sequence objects and open squares represent objects unrelated to Chamaeleon I (Alcalá et al. 1995); and (*f*) a map of the average $H-K_s$ stellar color with $5'$ resolution, where the contour levels are at 0.20, 0.35, 0.50 mag, and increments of 0.30 mag thereafter. These panels show that the largest concentration of variable stars is toward the Chamaeleon I molecular cloud despite the overall decrease in the stellar surface density, indicating many of the variable stars must be associated with the Chamaeleon I molecular cloud.

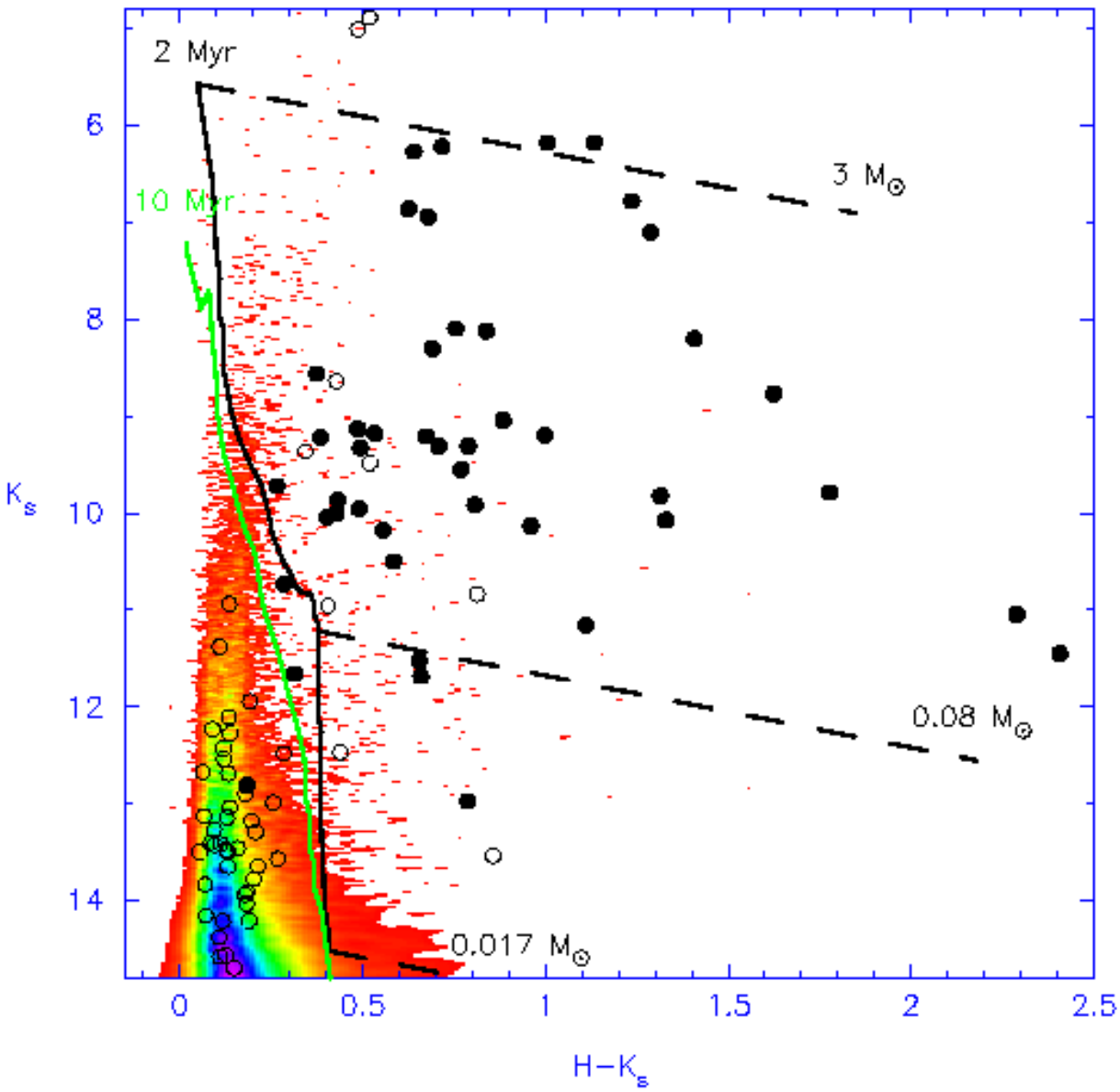

Fig. 5.— K_s vs. $H - K_s$ color-magnitude diagram for all stars (color scale) and the variable stars (circles). Filled circles indicate stars which have been previously identified as members of Chamaeleon I. The solid black curve shows the 2 Myr pre-main-sequence isochrone from D'Antona & Mazzitelli (1997,98) for masses between $0.017\,M_\odot$ and $3.0\,M_\odot$, and the green curve shows the 10 Myr isochrone. The dashed lines indicate the reddening vector for 10 magnitudes of visual extinction from Cohen et al. (1981) transformed into the 2MASS photometric system (Carpenter 2001), where the reddening vector is drawn at 0.017, 0.08, and $3.0\,M_\odot$. This figure shows that a large number of the variable stars are consistent with reddened pre-main-sequence stars with masses $\lesssim 3\,M_\odot$. A second group of variable stars are faint and blue, and as discussed in the text, are most likely variable field stars or old pre-main-sequence stars unrelated to Chamaeleon I.

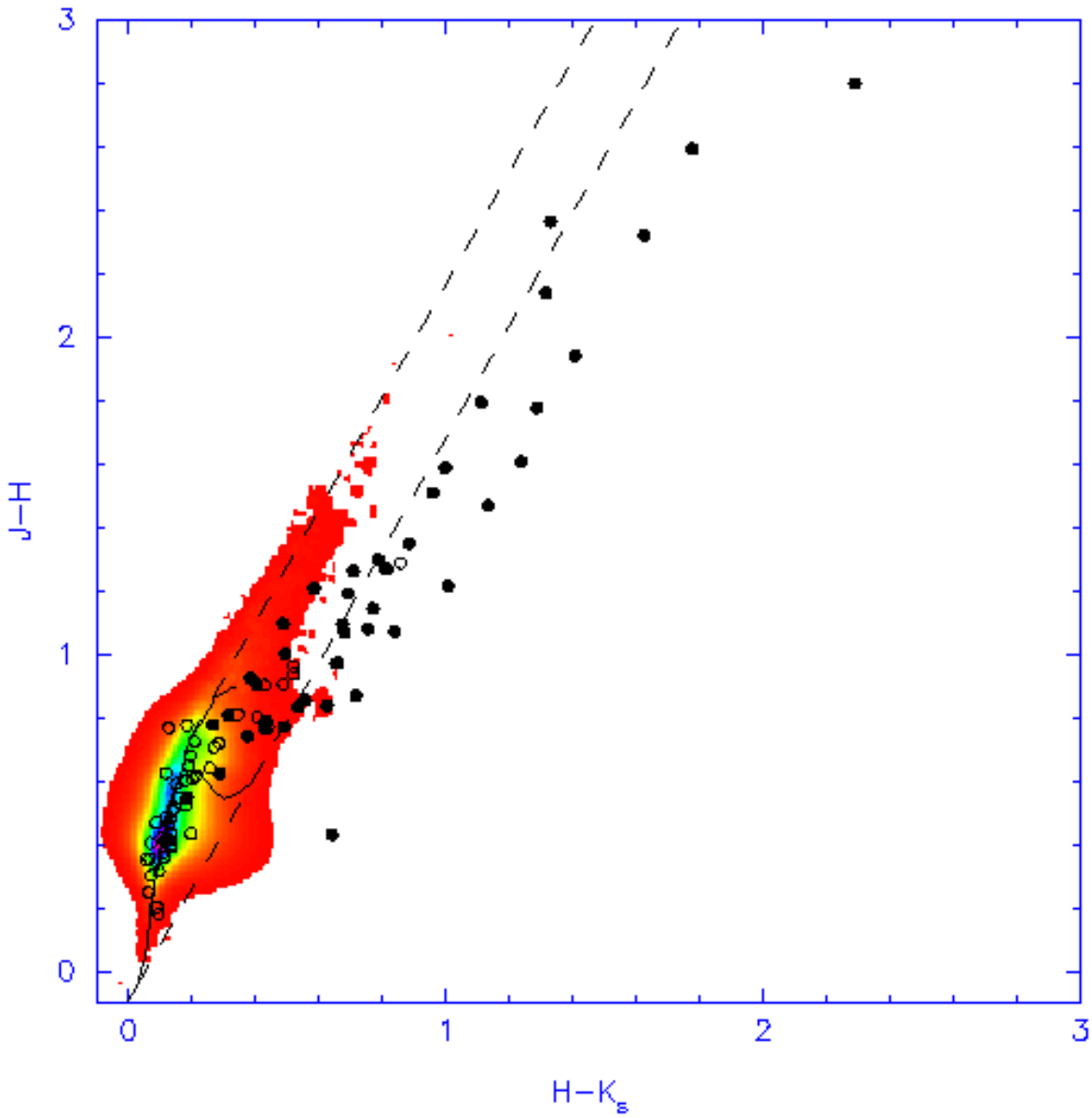

Fig. 6.— $J - H$ vs. $H - K_s$ color-color diagram for all stars (color scale) and the 95 variable stars (circles) identified from the J, H, and K_s time-series data. The filled circles represent variable stars that were previously identified as likely Chamaeleon I members.

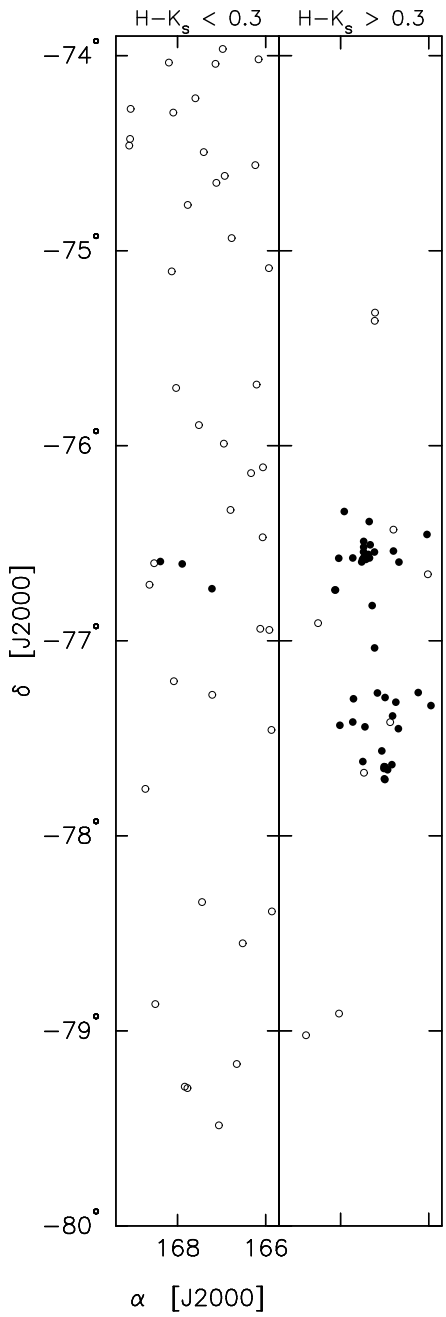

Fig. 7.— Spatial distribution of variable stars for two different color ranges. The left panel shows the distribution of relatively blue variables with $H - K_s < 0.3$, and the right panel shows the distribution of red variables with $H - K_s > 0.3$. The blue variable stars are found over the entire region, while the red variable stars, not surprisingly, are located mainly toward the molecular cloud. Of the 4 red variable stars found well outside the cloud boundaries, one is thought to be a Mira variable, one is a known pre-main-sequence star identified from the ROSAT All Sky Survey (Alcalá et al. 1995), and the remaining 2 are of unknown origin. As discussed in the text, the faint, blue variable stars are most likely field stars or an older population (> 10 Myr) of low mass pre-main-sequence stars located beyond the Chamaeleon I cloud.

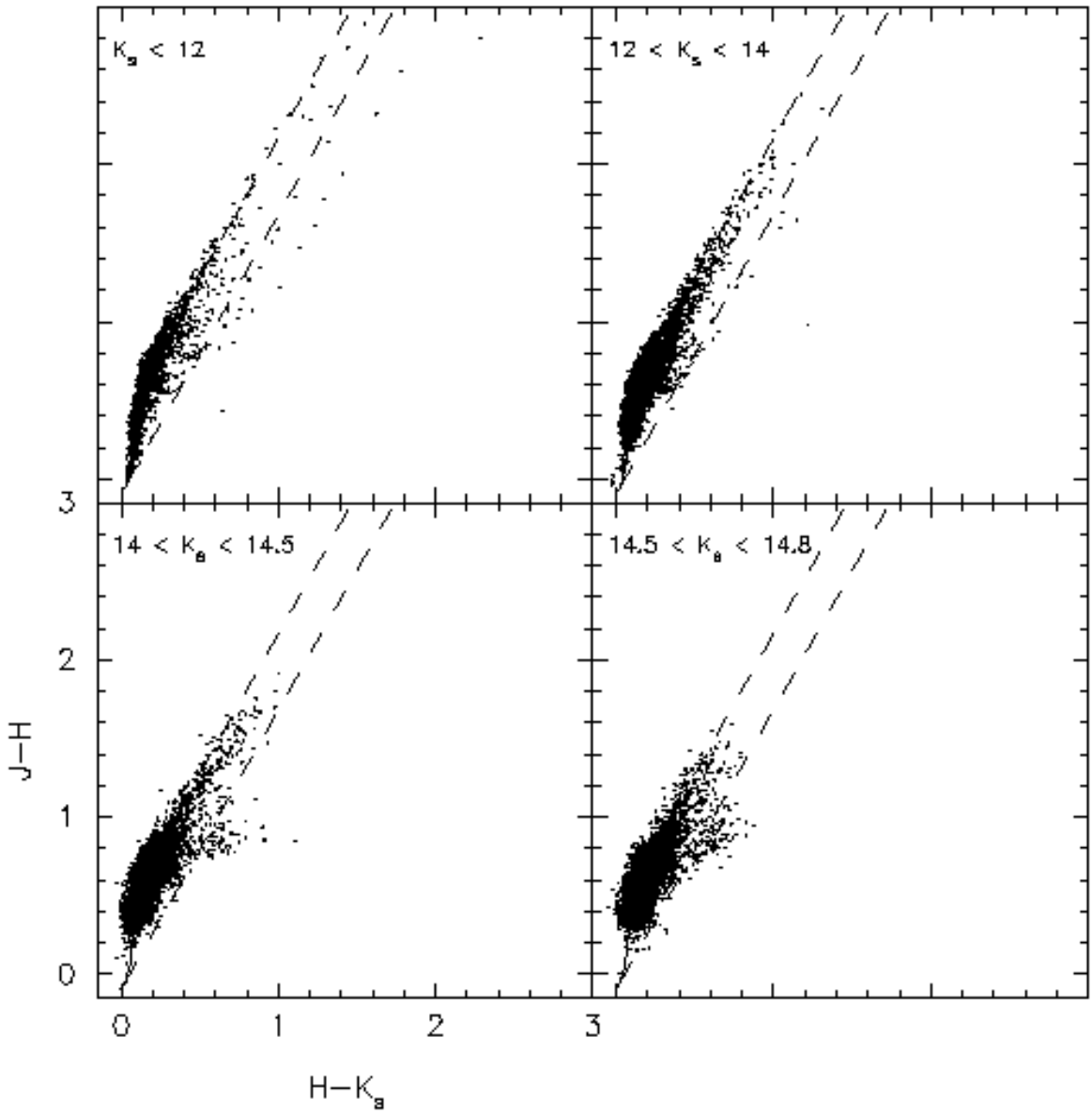

Fig. 8.— $J-H$ vs. $H-K_s$ color-color diagrams in four different K_s-band magnitude intervals for objects in the source list with at least 10 $J-H$ and $H-K_s$ measurements. The number of sources shown in each panel are 2869 for $K_s < 12$, 10070 for $12 < K_s < 14$, 6336 for $14 < K_s < 14.5$ and 5320 for $14.5 < K_s < 14.8$. Sources with a near-infrared excess and brighter than K_s=14 are most likely stars associated with Chamaeleon I and surrounded by an accretion disk. The fainter sources with an infrared excess are most likely galaxies with redshifts of $z \lesssim 0.25$ as discussed in the text.

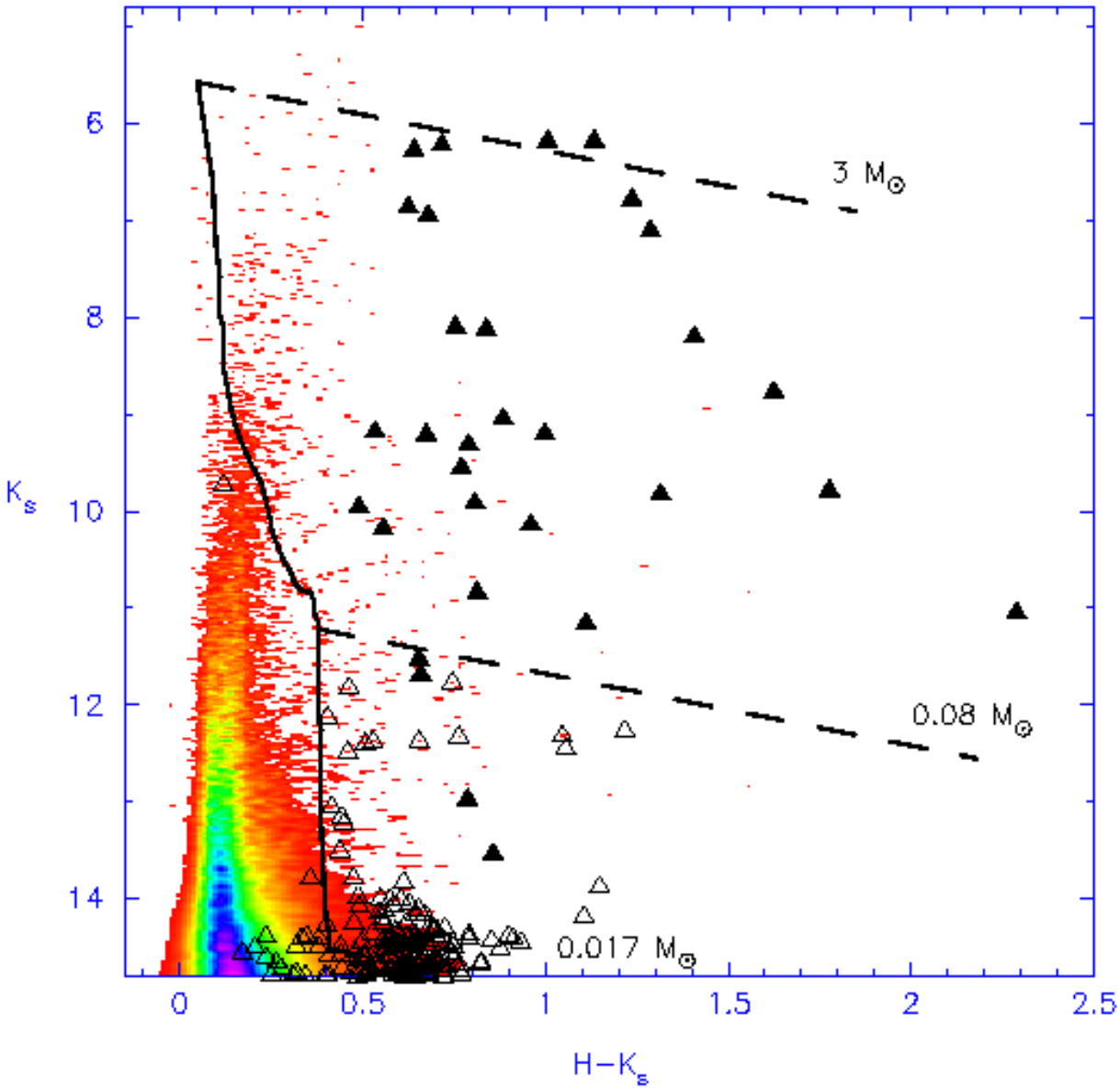

Fig. 9.— K_s vs. $H - K_s$ color-magnitude diagram for all sources (color scale) and sources with a near-infrared excess (triangles) detectable in the $J - H$ vs. $H - K_s$ color-color diagram. Filled triangles represent the subset of sources with excesses that are also variable. Sources with excesses and brighter than K_s=13.5 (see Fig. 4) are clustered around the Chamaeleon I molecular cloud and are most likely pre-main-sequence stars (for $K_s \lesssim 11$) and brown dwarf candidates (for $11 \lesssim K_s \lesssim 13.5$). Objects fainter than $K_s = 13.5$ are distributed over the entire survey area and are most likely galaxies as discussed in the text.

# Name	RA(J2000)	Dec(J2000)	2MASS	Cam98	GCVS	W87	Sz77	Hoff63	HM73	F93	FK89	Hn93	H82/J85	HBC88	P00	KG01	GK01	OTS99	B84	IRAS	Other
T_1	10:52:01.30	-77:09:50.1	WDB	Cam1 1	------	T 1	Sz 1	------	-------	---------	-------	------	------	-------	-------	------	------	------	-----	----------	
IRAS_10529-7638	10:54:11.6	-76:54:33	-----	--------	------	-----	-----	------	-------	---------	-------	------	------	-------	-------	------	------	------	-----	10529-7638	
T_2	10:54:13.32	-77:55:09.2	WDB	Cam1 2	SW Cha	T 2	-----	S 6319	-------	---------	-------	------	------	-------	-------	------	------	------	-----	----------	
T_3	10:55:59.9	-77:24:38	-----	Cam1 3	SX Cha	T 3	Sz 2	S 6320	HM 1	---------	-------	------	------	HBC 564	-------	------	------	------	B 1	10548-7708	
T_4	10:56:30.43	-77:11:39.4	WDB	Cam1 4	SY Cha	T 4	Sz 3	S 6321	HM 2	CHXR 1	CHX 1	------	------	HBC 565	-------	------	------	------	B 2	10552-7655	
T_5	10:57:42.28	-76:59:35.7	WDB	Cam1 5	------	T 5	Sz 4	------	-------	---------	-------	------	------	-------	-------	------	------	------	-----	----------	
CHXR_3	10:58:05.61	-77:28:24.0	WDB	Cam1 6	------	-----	-----	------	-------	CHXR 3	-------	------	------	-------	-------	------	------	------	B 3	----------	
T_6	10:58:16.84	-77:17:17.1	WDB	Cam1 7	SZ Cha	T 6	-----	S 6323	-------	CHXR 4	CHX 2	------	------	HBC 566	-------	------	------	------	B 4	10570-7701	Glass V
T_7	10:59:01.15	-77:22:40.7	WDB	Cam1 8	TW Cha	T 7	Sz 5	S 6326	HM 3	CHXR 5	-------	------	------	HBC 567	-------	------	------	------	B 5	10577-7706	
T_8	10:59:07.00	-77:01:40.1	WDB	Cam1 9	CR Cha	T 8	Sz 6	------	HM 4	CHXR 6	CHX 3	------	------	HBC 244	-------	------	------	------	B 6	10578-7645	LkHa 332-20
T_9	11:00:14.08	-76:44:15.4	WDB	Cam1 10	------	T 9	Sz 7	------	HM 5	---------	-------	------	------	-------	-------	------	------	------	-----	10589-7628	
CHXR_8	11:00:14.54	-77:14:38.0	WDB	Cam1 11	------	-----	-----	------	-------	CHXR 8	-------	------	------	-------	-------	------	------	------	B 8	----------	
T_10	11:00:40.27	-76:19:28.0	WDB	Cam1 12	------	T 10	Sz 8	------	HM 6	---------	-------	------	------	-------	-------	------	------	------	-----	----------	
CHXR_9C	11:01:18.77	-76:27:02.5	WDB	Cam1 13	------	-----	-----	------	-------	CHXR 9C	-------	------	------	-------	-------	------	------	------	-----	----------	
B_23	11:01:46.6	-77:43:51	-----	--------	------	-----	-----	------	-------	---------	-------	------	------	-------	-------	------	------	------	B 23	----------	
B_9	11:02:15.4	-77:10:59	-----	Cam1 14	------	-----	-----	------	-------	---------	-------	------	------	-------	-------	------	------	------	B 9	----------	
ISO_1	11:02:16.3	-77:46:30	-----	--------	------	-----	-----	------	-------	---------	-------	------	------	-------	ISO 1	------	------	------	-----	----------	
T_11	11:02:24.92	-77:33:35.8	WDB	Cam1 15	CS Cha	T 11	Sz 9	------	HM 7	CHXR 10	CHX 4	------	------	HBC 569	ISO 3	------	------	------	B 10	11011-7717	
CHXR_71	11:02:32.67	-77:29:13.0	WDB	Cam1 16	------	-----	-----	------	-------	CHXR 71	-------	Hn 1	------	-------	ISO 4	------	------	------	B 11	----------	
ISO_13	11:02:53.1	-77:24:07	-----	--------	------	-----	-----	------	-------	---------	-------	------	------	-------	ISO 13	------	------	------	-----	----------	
T_12	11:02:55.06	-77:21:50.9	WDB	Cam1 17	------	T 12	Sz 10	------	HM 8	---------	-------	------	------	-------	-------	------	------	------	-----	----------	
CHXR_11	11:03:11.61	-77:21:04.3	WDB	Cam1 18	------	-----	-----	------	-------	CHXR 11	-------	------	------	-------	ISO 17	------	------	------	B 12	----------	
ISO_28	11:03:41.85	-77:26:52.1	757	--------	------	-----	-----	------	-------	---------	-------	------	------	-------	ISO 28	------	------	------	-----	----------	
Hn_2	11:03:47.66	-77:19:56.4	1012	Cam1 19	------	-----	-----	------	-------	---------	-------	Hn 2	------	-------	ISO 32	------	------	------	B 13a	----------	
T_13	11:03:51.01	-76:55:45.6	1154	Cam1 20	TZ Cha	T 13	-----	S 6334	-------	---------	-------	------	------	-------	-------	------	------	------	-----	----------	
CHXR_12	11:03:56.83	-77:21:33.0	1403	Cam1 21	------	-----	-----	------	-------	CHXR 12	-------	Hn 3	------	-------	ISO 34	------	------	------	B 14	----------	
T_14	11:04:09.11	-76:27:19.3	1898	Cam1 22	CT Cha	T 14	Sz 11	------	HM 9	CHXR 13	-------	------	------	HBC 570	-------	------	------	------	-----	11027-7611	
CHXR_72	11:04:11.06	-76:54:32.2	2002	Cam1 23	------	-----	-----	------	-------	CHXR 72	-------	------	------	-------	-------	------	------	------	-----	----------	
T_14a	11:04:22.78	-77:18:08.2	2482	Cam1 24	------	T 14a	-----	------	-------	---------	-------	------	------	-------	ISO 46	------	------	------	-----	11030-7702	HH 48
T_15	11:04:24.26	-77:25:48.8	2553	Cam1 25	------	T 15	Sz 12	------	HM 10	---------	-------	------	------	-------	ISO 48	------	------	------	-----	----------	
ISO_52	11:04:42.59	-77:41:57.1	3319	Cam1 26	------	-----	-----	------	-------	---------	-------	------	------	-------	ISO 52	------	------	------	B 18	----------	
CHXR_14N	11:04:51.03	-76:25:24.0	3657	Cam1 27	------	-----	-----	------	-------	CHXR 14N	-------	------	------	-------	-------	------	------	------	-----	----------	
CHXR_14S	11:04:52.87	-76:25:51.5	3716	Cam1 28	------	-----	-----	------	-------	CHXR 14S	-------	------	------	-------	-------	------	------	------	-----	----------	
T_16	11:04:57.00	-77:15:57.0	3876	Cam1 29	------	T 16	Sz 13	------	-------	---------	-------	------	------	-------	ISO 55	------	------	------	B 19	----------	
B_29	11:05:01.9	-77:41:31	-----	--------	------	-----	-----	------	-------	---------	-------	------	------	-------	-------	------	------	------	B 29	----------	
Hn_4	11:05:14.64	-77:11:29.2	4629	Cam1 30	------	-----	-----	------	-------	---------	-------	Hn 4	------	-------	-------	------	------	------	-----	----------	
T_18	11:05:15.23	-77:52:54.7	4649	Cam1 31	------	T 18	Sz 14	------	-------	---------	-------	------	------	-------	-------	------	------	------	-----	----------	
T_17	11:05:21.60	-76:30:21.6	4943	Cam1 32	UU Cha	T 17	-----	S 6335	-------	---------	-------	------	------	-------	-------	------	------	------	-----	----------	
T_19	11:05:41.57	-77:54:44.0	5797	Cam1 33	------	T 19	Sz 15	------	-------	---------	-------	------	------	-------	-------	------	------	------	-----	----------	
CHXR_15	11:05:42.97	-77:26:51.7	5856	Cam1 34	------	-----	-----	------	-------	CHXR 15	-------	------	------	-------	ISO 65	------	------	------	B 22	----------	
T_20	11:05:52.62	-76:18:25.5	6267	Cam1 35	UV Cha	T 20	-----	S 6336	-------	CHXR 18	-------	------	------	HBC 571	-------	------	------	------	-----	----------	
ISO_68	11:05:53.93	-77:43:27.2	6314	--------	------	-----	-----	------	-------	---------	-------	------	------	-------	ISO 68	------	------	------	-----	----------	
ISO_71	11:06:04.06	-77:39:23.8	6738	--------	------	-----	-----	------	-------	---------	-------	------	------	-------	ISO 71	------	------	------	-----	----------	
T_21	11:06:15.36	-77:21:56.7	7184	Cam1 36	------	T 21	-----	------	-------	CHXR 19	CHX 7	------	------	-------	ISO 75	------	------	------	-----	11048-7706	Glass F,Ced 110,Ced 110 IRS2
B_31	11:06:26.4	-77:34:20	-----	--------	------	-----	-----	------	-------	---------	-------	------	------	-------	-------	------	------	------	B 31	----------	
CHXR_73	11:06:28.72	-77:37:33.2	7730	--------	------	-----	-----	------	-------	CHXR 73	-------	------	------	-------	ISO 78	------	------	------	B 25	----------	
Cha_Ha_12	11:06:37.93	-77:43:09.2	8077	--------	------	-----	-----	------	-------	---------	-------	------	------	-------	-------	------	------	------	-----	----------	
ISO_79	11:06:39.42	-77:36:05.3	8134	--------	------	-----	-----	------	-------	---------	-------	------	------	-------	ISO 79	------	GK 13	------	-----	----------	
Hn_5	11:06:41.76	-76:35:49.2	8234	Cam1 37	------	-----	-----	------	-------	---------	-------	Hn 5	------	-------	-------	------	------	------	-----	----------	
T_22	11:06:43.43	-77:26:34.5	8284	Cam1 38	UX Cha	T 22	-----	S 6337	-------	---------	-------	------	------	-------	ISO 80	------	------	------	-----	----------	
CHXR_20	11:06:45.05	-77:27:02.5	8369	Cam1 39	------	-----	-----	------	-------	CHXR 20	CHX 8	------	------	-------	ISO 81	------	------	------	B 26	----------	Ced 110 IRS3
Ced_110_IRS4	11:06:46.23	-77:22:29.0	8415	Cam1 40	------	-----	-----	------	-------	---------	-------	------	------	-------	ISO 84	------	------	------	-----	11051-7706	Ced 110 IRS4
CHXR_74	11:06:57.29	-77:42:10.6	8892	--------	------	-----	-----	------	-------	CHXR 74	-------	------	------	-------	ISO 87	------	------	------	B 27	----------	
ISO_86	11:06:58.01	-77:22:48.8	8924	--------	------	-----	-----	------	-------	---------	-------	------	------	-------	ISO 86	------	------	------	-----	----------	
T_23	11:06:59.01	-77:18:53.5	8978	Cam1 41	UY Cha	T 23	Sz 16	S 6340	HM 11	---------	-------	------	------	-------	ISO 89	------	------	------	-----	----------	Ced 110 IRS5
Ced_110_IRS6	11:07:09.15	-77:23:05.0	9387	Cam1 42	------	-----	-----	------	-------	---------	-------	------	------	-------	ISO 92	------	------	------	-----	11057-7706	Ced 110 IRS6
ISO_91	11:07:09.19	-77:18:47.1	9391	Cam2 21	------	-----	-----	------	-------	---------	-------	------	------	-------	ISO 91	------	------	------	-----	----------	
CHXR_22W	11:07:10.42	-77:43:44.2	9433	Cam1 43	------	-----	-----	------	-------	CHXR 22W	-------	------	------	-------	ISO 93	------	------	------	-----	----------	
CHXR_21	11:07:11.43	-77:46:39.4	9467	Cam1 44	------	-----	-----	------	-------	CHXR 21	-------	Hn 6	------	-------	ISO 94	KG 1	------	------	B 28	----------	
T_24	11:07:12.04	-76:32:23.3	9496	Cam1 45	UZ Cha	T 24	Sz 17	S 6341	-------	CHXR 75	-------	------	------	-------	-------	------	------	------	-----	----------	
CHXR_22E	11:07:13.27	-77:43:49.8	9542	Cam1 46	------	-----	-----	------	-------	CHXR 22E	-------	------	------	-------	-------	KG 2	------	------	B 29	----------	
ISO_97	11:07:16.19	-77:23:06.9	9652	Cam2 23	------	-----	-----	------	-------	---------	-------	------	------	-------	ISO 97	KG 3	------	------	-----	----------	
Cha_Ha_1	11:07:16.65	-77:35:53.3	9671	--------	------	-----	-----	------	-------	---------	-------	------	------	-------	ISO 95	------	------	------	-----	----------	
Cha_Ha_9	11:07:18.56	-77:32:51.6	9753	--------	------	-----	-----	------	-------	---------	-------	------	------	-------	ISO 98	------	------	------	-----	----------	
T_25	11:07:19.15	-76:03:04.9	9782	Cam1 47	------	T 25	Sz 18	------	HM 12	---------	-------	------	------	HBC 572	-------	------	------	------	-----	11057-7546	
T_26	11:07:20.72	-77:38:07.3	9847	Cam1 48	DI Cha	T 26	Sz 19	------	HM 13	CHXR 23	CHX 9	------	------	HBC 245	ISO 100	KG 6	------	------	B 32	11059-7721	LkHa 332-17,Ced 111 IRS1
B_35	11:07:21.38	-77:22:11.8	9872	Cam2 24	------	-----	-----	------	-------	---------	-------	------	------	-------	ISO 101	KG 7	------	------	B 35	----------	
T_27	11:07:28.24	-76:52:11.9	10138	Cam1 49	VV Cha	T 27	Sz 20	S 6342	HM 14	CHXR 24	-------	------	------	HBC 573	-------	KG 12	------	------	-----	----------	
CHXR_25	11:07:32.97	-77:28:27.9	10307	Cam1 50	------	-----	-----	------	-------	CHXR 25	-------	------	------	-------	ISO 105	KG 13	------	------	B 33	----------	
CHXR_76	11:07:35.16	-77:34:49.5	10394	Cam1 51	------	-----	-----	------	-------	CHXR 76	-------	------	------	-------	ISO 106	KG 15	------	------	B 34	----------	
CHXR_26	11:07:36.84	-77:33:33.6	10464	Cam1 52	------	-----	-----	------	-------	CHXR 26	-------	------	------	-------	ISO 108	KG 17	------	------	B 35	----------	
Cha_Ha_7	11:07:37.72	-77:35:31.0	10496	Cam2 26	------	-----	-----	------	-------	---------	-------	------	------	-------	-------	------	------	------	-----	----------	
Cha_Ha_2	11:07:42.44	-77:33:59.6	10685	--------	------	-----	-----	------	-------	---------	-------	------	------	-------	ISO 111	KG 20	------	------	-----	----------	
T_28	11:07:43.64	-77:39:41.2	10737	Cam1 53	------	T 28	Sz 21	------	HM 15	CHXR 27	-------	------	------	HBC 574	ISO 112	KG 21	------	------	B 36	----------	
Cha_Ha_8	11:07:46.07	-77:40:09.0	10837	--------	------	-----	-----	------	-------	---------	-------	------	------	-------	-------	------	------	------	-----	----------	
ISO_114	11:07:51.15	-77:10:00.1	11070	--------	------	-----	-----	------	-------	---------	-------	------	------	-------	ISO 114	------	------	------	-----	----------	

Cha_Ha_3	11:07:52.24	-77:36:57.2	11114														ISO	116	KG	23					
CHXR_28	11:07:55.85	-77:27:25.9	11256	Cam1	54						CHXR 28	CHX 10a					ISO	117	KG	24			B	37	
CHXR_30b	11:07:57.28	-77:17:26.4	11315	Cam1	55						CHXR 30b								KG	26			B	38b	11065-7701 Ced 110 IRS7
T_29	11:07:57.91	-77:38:45.1	11344	Cam1	56	T	29	Sz 22		HM 16							ISO	119	KG	28			B	39	
T_30	11:07:58.07	-77:42:41.4	11351	Cam1	57	T	30	Sz 23									ISO	120	KG	27					
CHXR_30a	11:07:59.98	-77:17:30.6	11416	Cam1	58						CHXR 30a						ISO	122	KG	30			B	38a	
T_31	11:08:01.47	-77:42:28.9	11462	Cam1	59	VW Cha	T	31	Sz 24	S 6343	HM 17	CHXR 31	CHX 11			HBC 575	ISO	123	KG	31			B	40	Ced 111 IRS3
ISO_126	11:08:02.93	-77:38:42.8	11529	Cam2	32												ISO	126	KG	33					
T_32	11:08:03.26	-77:39:17.6	11547	Cam1	60	CU Cha	T	32	Sz 25		HM 18	CHXR 29				HBC 246	ISO	124	KG	34					11066-7722 HD 97048,Ced 111 IRS2
T_33	11:08:15.33	-77:33:53.5	12055	Cam1	61		T	33				CHXR 32	CHX 12				ISO	135	KG	39			B	42	11068-7717 Glass I,Ced 111 IRS4
T_34	11:08:16.46	-77:44:37.3	12090	Cam1	62		T	34	Sz 26		HM 19						ISO	136	KG	40			B	44	
Cha_Ha_13	11:08:17.01	-77:44:12.0	12108														ISO	137	KG	41					
B_40	11:08:17.9	-77:32:22																					B	40	
ISO_138	11:08:18.44	-77:30:41.0	12159														ISO	138							
Cha_Ha_4	11:08:18.93	-77:39:17.3	12180																						
ISO_143	11:08:22.33	-77:30:27.9	12355														ISO	143	KG	45					
Cha_Ha_10	11:08:24.02	-77:39:30.2	12438																						
Cha_Ha_5	11:08:24.08	-77:41:47.6	12442														ISO	144	KG	47					
ISO_145	11:08:25.77	-76:55:57.0	12496														ISO	145							
ISO_147	11:08:26.45	-77:15:55.2	12525														ISO	147							
Cha_Ha_11	11:08:29.23	-77:39:19.9	12653																						
IRN	11:08:38.95	-77:43:51.4	13053	Cam1	63												ISO	150	KG	49					11072-7727 IRN,Ced 111 IRS5
T_35	11:08:39.01	-77:16:04.2	13058	Cam1	64		T	35	Sz 27		HM 20				C6-1	HBC 576	ISO	151	KG	50					Ced 110 IRS8
Cha_Ha_6	11:08:39.49	-77:34:16.8	13082														ISO	152	KG	51					
CHXR_33	11:08:40.70	-76:36:07.9	13131	Cam1	65							CHXR 33	CHX 13a		C1-10		ISO	153	KG	52					
ISO_154	11:08:43.05	-76:27:46.8	13217														ISO	154							
T_37	11:08:50.92	-76:25:13.7	13553	Cam1	68		T	37	Sz 28								ISO	157	KG	54					
T_36	11:08:52.36	-76:43:59.6	13616	Cam1	66	VX Cha	T	36		S 6345															
CHXR_78C	11:08:54.19	-77:32:11.7	13696	Cam1	69							CHXR 78C					ISO	160	KG	56			B	45	
T_38	11:08:54.61	-77:02:13.1	13707	Cam1	70	VY Cha	T	38	Sz 29	S 6346	HM 21				C4-5	HBC 577	ISO	162	KG	58					
ISO_164	11:08:54.75	-76:39:41.6	13713														ISO	164							
ISO_165	11:08:54.98	-76:32:41.2	13720														ISO	165	KG	59					
Hn_7	11:09:05.10	-77:09:58.0	14124	Cam1	71									Hn 7			ISO	174							
ISO_177	11:09:07.92	-76:49:10.6	14235														ISO	177	KG	71					
T_39	11:09:11.71	-77:29:12.6	14388	Cam1	72		T	39	Sz 30			CHXR 36	CHX 14		C7-7		ISO	182	KG	74			B	46	
CHXR_35	11:09:13.84	-76:28:39.6	14469	Cam1	73							CHXR 35		Hn 8	C1-15				KG	75					
OTS_7	11:09:16.5	-76:36:39																			OTS	7			
CHXR_37	11:09:17.72	-76:27:57.8	14604	Cam1	74							CHXR 37					ISO	185	KG	77					
CHXR_79	11:09:18.15	-76:30:29.3	14623	Cam1	75							CHXR 79		Hn 9	C1-18		ISO	186	KG	79					
C_1-6	11:09:22.67	-76:34:32.1	14800	Cam1	76										C1-6		ISO	189	KG	82	OTS	10			
T_40	11:09:23.80	-76:23:20.8	14843	Cam1	77	VZ Cha	T	40	Sz 31	S 6347	HM 22	CHXR 39				HBC 578			KG	83					11078-7607 Ced 112 IRS1
OTS_11	11:09:24.1	-76:34:55																	GK	82	OTS	11			
Ced_112_IRS2	11:09:26.05	-76:33:33.8	14947	Cam2	40										C1-3				KG	85	OTS	13			Ced 112 IRS2
ISO_192	11:09:28.55	-76:33:28.1	15044	Cam2	41												ISO	192	KG	87	OTS	15			
CHXR_40	11:09:40.08	-76:28:39.2	15504	Cam1	78							CHXR 40	CHX 15b				ISO	198	KG	92					
C_1-25	11:09:41.91	-76:34:58.5	15576	Cam1	79										C1-25		ISO	199	KG	93	OTS	19			
C_7-1	11:09:42.55	-77:25:58.0	15600	Cam1	80										C7-1		ISO	200	KG	95					Ced 110 IRS9
Hn_10W	11:09:43.07	-76:34:38.7	15622	Cam1	83									Hn 10W							OTS	20			
C_2-3	11:09:45.86	-76:43:54.5	15732	Cam1	81										C2-3		ISO	203	KG	99					
Hn_10E	11:09:46.19	-76:34:46.5	15745	Cam1	82		T	42	Sz 32		HM 23			Hn 10E	C1-24		ISO	204	KG	97	OTS	24			11083-7618 Ced 112 IRS4
B_43	11:09:47.37	-77:26:29.3	15784	Cam1	84												ISO	207	KG	101			B	43	
ISO_206	11:09:47.63	-76:51:18.2	15796														ISO	206							
ISO_209	11:09:48.62	-77:14:38.4	15850	Cam2	45												ISO	209							
T_41	11:09:50.01	-76:36:47.7	15900	Cam1	85		T	41				CHXR 42			C1-11		ISO	211	KG	103	OTS	26			11082-7620 HD 97300,Ced 112 IRS3
ISO_216	11:09:51.98	-76:57:58.9	15973												C4-1		ISO	216	KG	107					
ISO_217	11:09:52.14	-76:39:12.8	15980														ISO	217	KG	106	GK	29			
ISO_220	11:09:53.31	-77:28:36.7	16023														ISO	220			GK	30			
T_42	11:09:53.40	-76:34:25.6	16026	Cam1	86		T	42	Sz 32		HM 23				C1-5	HBC 579	ISO	223	KG	109	OTS	27			11083-7618
T_43	11:09:54.06	-76:29:25.4	16052	Cam1	87		T	43	Sz 33			CHXR 41	CHX 15		C1-17		ISO	224	KG	110					
ISO_225	11:09:54.38	-76:31:11.4	16067														ISO	225			GK	31			
C_1-2	11:09:55.05	-76:32:41.1	16096	Cam1	88										C1-2		ISO	226	KG	111	OTS	28			Ced 112 IRS5
T_45	11:09:58.68	-77:37:09.1	16254	Cam1	89	WX Cha	T	45	Sz 35	S 6349	HM 25	CHXR 43	CHX 17		C8-3	HBC 581	ISO	228	KG	114			B	48	11085-7720 Ced 111 IRS6
T_44	11:10:00.09	-76:34:57.9	16307	Cam1	90	WW Cha	T	44	Sz 34	S 6348	HM 24	CHXR 44			C1-7	HBC 580	ISO	231	KG	116	OTS	29			
OTS_31	11:10:02.4	-76:32:37																			OTS	31			
OTS_32	11:10:03.35	-76:33:11.1	16422																		OTS	32			
Hn_11	11:10:03.69	-76:33:29.2	16436	Cam1	91									Hn 11	C1-4		ISO	232	KG	117	OTS	33			
T_45a	11:10:04.68	-76:35:45.2	16470	Cam1	92		T	45a				CHXR 45	CHX 16		C1-9	HBC 582	ISO	233	KG	118	OTS	35			GK-1
T_46	11:10:07.04	-76:29:37.6	16560	Cam1	93	WY Cha	T	46	Sz 36	S 6351	HM 26	CHXR 46			C1-16	HBC 583	ISO	234	KG	119					11085-7613 Ced 112 IRS6
ISO_235	11:10:07.83	-77:27:48.1	16611														ISO	235	KG	120					
OTS_44	11:10:09.32	-76:32:18.0	16658																		OTS	44			
OTS_42	11:10:09.34	-76:35:06.4	16659																		OTS	42			
ISO_237	11:10:11.40	-76:35:29.2	16751	Cam2	48										C1-8		ISO	237	KG	121	OTS	45			
OTS_48	11:10:14.1	-76:34:37																			OTS	48			
Hn_12W	11:10:28.50	-77:16:59.6	17417	Cam1	94									Hn 12W	C6-2		ISO	244							
OTS_56	11:10:30.0	-76:32:53																			OTS	56			
Hn_12E	11:10:30.67	-77:17:00.9	17515	Cam1	95									Hn 12E											
OTS_59	11:10:32.0	-76:35:55																			OTS	59			

ISO_247	11:10:33.68	-76:39:22.4	17625	--------	------	-----	-----	------	-------	---------	-------	------	------	-------	ISO 247	------	------	------	-----	----------			
ISO_250	11:10:36.42	-77:22:13.1	17743	--------	------	-----	-----	------	-------	---------	-------	------	------	-------	ISO 250	------	------	------	-----	----------			
CHXR_47	11:10:38.00	-77:32:40.0	17807	Cam1	96	------	F 34	-----	------	-------	CHXR 47	-------	------	C7-11	-------	ISO 251	KG 124	------	------	B 50	11091-7716	Glass Q,Ced 111 IRS7	
ISO_252	11:10:41.40	-77:20:48.1	17959	--------	------	-----	-----	------	-------	---------	-------	------	------	-------	ISO 252	------	------	------	-----	----------			
OTS_61	11:10:42.9	-76:34:05	-----	--------	------	-----	-----	------	-------	---------	-------	------	------	-------	-------	------	------	OTS 61	-----	----------			
T_47	11:10:49.57	-77:17:51.8	18261	Cam1	97	------	T 47	Sz 37	------	HM 27	---------	-------	------	------	HBC 584	ISO 254	------	------	------	-----	11093-7701		
T_48	11:10:53.33	-76:34:32.0	18403	Cam1	98	WZ Cha	T 48	Sz 38	S 6352	HM 28	CHXR 82	-------	------	C1-23	HBC 585	ISO 258	------	------	------	-----	----------		
ISO_256	11:10:53.58	-77:25:00.6	18416	Cam2	49	------	-----	-----	------	-------	---------	-------	------	------	-------	ISO 256	------	------	------	-----	----------		
Hn_13	11:10:55.96	-76:45:32.6	18502	Cam1	99	------	-----	-----	------	-------	---------	-------	Hn 13	C2-5	-------	ISO 259	------	------	------	-----	----------		
B_47	11:11:09.1	-77:26:19	-----	--------	------	-----	-----	------	-------	---------	-------	------	------	-------	-------	------	------	------	B 47	----------			
Hn_14	11:11:14.17	-76:41:11.1	19316	Cam1	100	------	-----	-----	------	-------	---------	-------	Hn 14	------	-------	-------	------	------	------	-----	----------		
ISO_274	11:11:25.48	-77:06:10.2	19793	--------	------	-----	-----	------	-------	---------	-------	------	------	-------	ISO 274	------	------	------	-----	----------			
CHXR_48	11:11:34.74	-76:36:21.3	20217	Cam1	101	------	-----	-----	------	-------	CHXR 48	-------	------	E1-7	-------	ISO 280	------	------	------	-----	----------		
T_49	11:11:39.67	-76:20:15.1	20409	Cam1	102	XX Cha	T 49	Sz 39	------	HM 29	---------	-------	------	------	HBC 586	-------	------	------	------	-----	11101-7603		
CHX_18N	11:11:46.34	-76:20:09.0	20702	Cam1	103	------	-----	-----	------	-------	---------	CHX 18N	------	------	-------	-------	------	------	------	-----	11101-7603		
CHXR_49NE	11:11:54.01	-76:19:30.9	21078	Cam1	104	------	-----	-----	------	-------	CHXR 49NE	CHX 18	Hn 15	------	-------	-------	------	------	------	-----	----------		
CHXR_84	11:12:03.28	-76:37:03.3	21466	Cam1	105	------	-----	-----	------	-------	CHXR 84	-------	Hn 16	E1-10	-------	-------	------	------	------	-----	----------		
ISO_282	11:12:03.50	-77:26:00.9	21473	--------	------	-----	-----	------	-------	---------	-------	------	------	-------	ISO 282	------	------	------	-----	----------			
T_50	11:12:09.84	-76:34:36.6	21745	Cam1	106	------	T 50	Sz 40	------	-------	CHXR 85	-------	------	E1-5	HBC 587	-------	------	------	------	-----	----------		
T_51	11:12:24.41	-76:37:06.5	22361	Cam1	107	------	T 51	Sz 41	------	-------	CHXR 50	CHX 20b	------	E1-9a	HBC 588	-------	------	------	------	-----	11108-7620	Ced 112 IRS7	
T_52	11:12:27.71	-76:44:22.4	22521	Cam1	108	CV Cha	T 52	Sz 42	------	HM 30	CHXR 51	CHX 19	------	E2-4	HBC 247	-------	------	------	------	-----	11108-7627	LkHa 332-21,Ced 112 IRS8	
CHXR_53	11:12:27.75	-76:25:29.3	22524	Cam1	109	------	-----	-----	------	-------	CHXR 53	-------	------	------	-------	-------	------	------	------	-----	----------		
T_53	11:12:30.93	-76:44:24.1	22662	Cam1	110	CW Cha	T 53	Sz 43	------	HM 31	---------	-------	------	------	HBC 589	-------	------	------	------	-----	----------		
CHXR_54	11:12:42.10	-76:58:40.1	23146	Cam1	111	------	-----	-----	------	-------	CHXR 54	CHX 21a	------	E4-3	-------	-------	------	------	------	-----	----------		
T_54	11:12:42.67	-77:22:23.0	23172	Cam1	112	------	T 54	-----	------	HM Anon	CHXR 56	CHX 22	------	------	-------	-------	------	------	B 51	11111-7705			
CHXR_55	11:12:42.98	-76:37:05.0	23183	Cam1	113	------	-----	-----	------	-------	CHXR 55	CHX 20E	------	E1-8	-------	-------	------	------	------	-----	----------		
Hn_17	11:12:48.59	-76:47:06.7	23447	Cam1	114	------	-----	-----	------	-------	---------	-------	Hn 17	E2-9	-------	-------	------	------	------	-----	----------		
CHXR_57	11:13:20.13	-77:01:04.4	24835	Cam1	115	------	-----	-----	------	-------	CHXR 57	-------	------	E4-4	-------	-------	------	------	B 52	----------			
Hn_18	11:13:24.45	-76:29:22.9	25026	Cam1	116	------	-----	-----	------	-------	---------	-------	Hn 18	------	-------	-------	------	------	------	-----	----------		
CHXR_59	11:13:27.36	-76:34:16.7	25148	Cam1	117	------	-----	-----	------	-------	CHXR 59	-------	------	E1-4	-------	-------	------	------	------	-----	----------		
CHXR_60	11:13:29.69	-76:29:01.4	25253	Cam1	118	------	-----	-----	------	-------	CHXR 60	-------	Hn 19	------	-------	-------	------	------	------	-----	----------		
IRAS_11120-7750	11:13:30.32	-78:07:02.4	25283	--------	------	-----	-----	------	-------	---------	-------	------	------	-------	-------	------	------	------	------	-----	11120-7750		
T_55	11:13:33.56	-76:35:37.5	25420	Cam1	119	------	T 55	Sz 44	------	-------	CHXR 61	-------	------	E1-6	-------	-------	------	------	------	-----	----------		
CHXR_62	11:14:15.64	-76:27:36.6	27295	Cam1	120	------	-----	-----	------	-------	CHXR 62	-------	Hn 20	------	-------	-------	------	------	------	-----	----------		
Hn_21W	11:14:24.50	-77:33:06.4	27714	Cam1	121	------	-----	-----	------	-------	---------	-------	Hn 21W	------	-------	-------	------	------	------	-----	----------		
Hn_21E	11:14:26.09	-77:33:04.4	27789	Cam1	122	------	-----	-----	------	-------	---------	-------	Hn 21E	------	-------	-------	------	------	------	-----	----------		
B_53	11:14:50.30	-77:33:38.8	28885	Cam1	123	------	-----	-----	------	-------	---------	-------	------	------	-------	-------	------	------	B 53	----------			
CHXR_65B	11:16:11.95	-77:14:10.1	32606	--------	------	-----	-----	------	-------	CHXR 65B	-------	------	------	------	-------	-------	------	------	------	-----	----------		
CHXR_65A	11:16:12.91	-77:14:06.5	32644	Cam1	124	------	-----	-----	------	-------	CHXR 65A	-------	------	------	-------	-------	------	------	B 54	----------			
T_56	11:17:36.95	-77:04:38.0	WDB	Cam1	125	------	T 56	Sz 45	------	HM 32	CHXR 66	-------	------	------	HBC 590	-------	------	------	------	-----	11159-7648		
CHXR_68B	11:18:19.54	-76:22:01.4	WDB	--------	------	-----	-----	------	-------	CHXR 68B	-------	------	------	-------	-------	------	------	------	------	-----	----------		
CHXR_68A	11:18:20.21	-76:21:57.7	WDB	Cam1	126	------	-----	-----	------	-------	CHXR 68A	-------	------	------	-------	-------	------	------	------	-----	----------		
IRAS_11248-7653	11:26:41.5	-77:10:15	-----	--------	------	-----	-----	------	-------	---------	-------	------	------	-------	-------	------	------	------	------	-----	11248-7653		